Zoology 124 (2017) 73–94

Contents lists available at ScienceDirect

Zoology

journal homepage: www.elsevier.com/locate/zool

Revisiting size and scaling in the anthropoid temporomandibular joint☆

Claire E. Terhune

Department of Anthropology, University of Arkansas, Old Main 330, Fayetteville, AR 72701, USA

ARTICLE INFO

Keywords:
Masticatory apparatus
Geometric morphometrics
Allometry
Temporomandibular joint morphology

ABSTRACT

Masticatory morphology in primates is likely under strong selective pressure to maximize feeding efficiency while simultaneously minimizing the occurrence of injury or pathology. As a result, masticatory shape, including aspects of temporomandibular joint (TMJ) morphology, varies widely across primates in relation to feeding behavior and body size. This study examines patterns of allometry in the TMJ of anthropoid primates, with the specific goal of evaluating how allometric patterns may reflect variation in loading and/or range of motion at this joint. Phylogenetic reduced major axis regressions were employed to examine how specific aspects of TMJ morphology scale in relation to body mass and mandible length. Patterns of shape variation across the entire masticatory apparatus were examined by utilizing geometric morphometric techniques. Results reveal that most aspects of TMJ shape scale with either isometry or positive allometry relative to body mass and/or mandible length, though several departures from these patterns were observed. In particular, male cercopithecoids tend to show distinct scaling patterns in TMJ height above the occlusal plane and condylar area, likely reflecting known trade-offs between increased range of motion and force production in this clade, as has been linked to selection for increased male canine size. The geometric morphometric analyses indicate that craniofacial and masticatory shape are strongly allometric, but that glenoid shape variation is less consistently allometric. Notably, different patterns of allometric shape variation were observed in platyrrhines, cercopithecoids, and hominoids, perhaps related to different, and potentially competing, selective pressures in each of these clades.

1. Introduction

The temporomandibular joint (TMJ) is arguably one of the most important, or at least one of the most frequently used, joints in the body (Moffett, 1966). As anyone who has experienced any form of TMJ disorder knows, problems with this joint make basic tasks such as eating, drinking, or speaking difficult. For a primate, damage that impairs the function of this joint − and thus feeding behaviors − can be problematic and have negative consequences on fitness. As a result, the form of the TMJ is likely under strong selective pressure to optimize masticatory function while minimizing the occurrence of injury or pathology, and multiple studies have demonstrated that the form of the mammalian TMJ varies in relation to feeding behavior (e.g., Maynard Smith and Savage, 1959; DuBrul, 1974; Herring and Herring, 1974; Hylander, 1975; Bouvier, 1986a,b; Wall, 1995; Vinyard, 1999; Vinyard et al., 2003; Norconk et al., 2009; Constantino, 2007; Terhune, 2011a,b; Terhune et al., 2015). Critically, feeding behaviors are strongly linked to body size (e.g., Kay, 1975a,b; Marshall and Wrangham, 2007; Ross et al., 2009a,b). As a result, masticatory morphology, including aspects of TMJ shape, also vary in relation to body size (e.g., Gould, 1975; Hylander, 1985; Bouvier, 1986a,b; Ravosa, 1996, 2000; Vinyard and Hanna, 2005; Taylor et al., 2015). However, while a variety of studies have assessed patterns of allometry in the masticatory apparatus, few researchers have specifically evaluated the shape of the primate TMJ relative to body and/or cranial size.

1.1. Masticatory scaling

There is a long history of analyses that evaluate how components of the masticatory apparatus scale across body sizes, taxonomic groups, and in relation to biomechanical demands (e.g., Hylander, 1975; Smith et al, 1983; Hylander, 1985; Bouvier, 1986a,b; Ravosa, 1996, 2000; Vinyard and Hanna, 2005; Taylor et al., 2015). Analyses of dental scaling patterns have identified a variety of allometric patterns across and among primate clades (e.g., Gould, 1975; Kay, 1975a,b; Corruccini and Henderson, 1978; Pirie, 1978; Vinyard and Hanna, 2005; Copes and Schwartz, 2010), though there is a general consensus that dental size varies consistently among dietary groups (i.e., among primates, frugivores have relatively smaller molars than insectivores and folivores) (e.g., Kay, 1975a,b; Kay and Hylander, 1978; Vinyard and Hanna, 2005; Scott, 2011, 2012).

Studies examining mandibular corpus and symphyseal size and shape suggest corpus robusticity and symphyseal thickness scale with positive allometry (e.g., Smith, 1983; Hylander, 1985; Ravosa, 1991;

☆ This article is part of a special issue entitled 'Determinants of Mammalian Feeding System Design'.

E-mail address: cterhune@uark.edu.

http://dx.doi.org/10.1016/j.zool.2017.08.005
Received 17 December 2016; Received in revised form 11 August 2017; Accepted 12 August 2017
Available online 18 August 2017
0944-2006/

Vinyard and Ravosa, 1998; Daegling, 2001), which has been linked to increased wishboning stresses along the lingual aspect of the mandibular symphysis. These patterns have also been linked to differences in dietary behaviors. For example, particular attention has been given to cercopithecoids, with folivorous colobines having anteroposteriorly shorter mandibles than frugivorous colobines at a given body size, and where colobines exhibit greater mandibular corpus depth than cercopithecines when these differences are examined relative to mandible length (e.g., Hylander, 1979; Bouvier, 1986a). These results have been used to suggest that colobine mandibles are better adapted to resisting increased stresses related to repeated cyclical loading (Hylander, 1979; Bouvier, 1986a). Complementary analyses emphasize the increased mechanical advantage of the masticatory apparatus in colobines relative to cercopithecines, suggesting that strong positive allometry of the facial skeleton helps cercopithecines achieve the large gapes (likely related to canine display behaviors) observed in this clade (Ravosa, 1990; Singleton, 2005; Hylander, 2013).

A number of researchers have also assessed scaling patterns in the masticatory musculature. Early work by Cachel (1984) and Antón (1999, 2000) suggested that muscle mass scales with isometry relative to body mass. Antón (1999, 2000) further found that mass of the macaque masseter and medial pterygoid muscles scaled with positive allometry relative to face size. More recent analyses (Anapol et al., 2008; Perry and Wall, 2008; Taylor and Vinyard, 2013; Taylor et al., 2015) have focused on muscle physiological cross-sectional area (PCSA), a measure that is proportional to the maximum force output of a given muscle (Powell et al., 1984). However, these analyses reveal somewhat conflicting patterns. Anapol et al. (2008) suggested a predominant pattern of positive allometry of PCSA relative to both body mass and cranial length across primates; Perry and Wall (2008) found isometry or slight positive allometry of prosimian PCSA relative to body mass; while Taylor and Vinyard (2013) identified isometry of PCSAs relative to jaw length in anthropoids, but positive allometry in hominoids. Furthermore, similar work by Taylor et al. (2015) found that, in platyrrhines, PCSA is negatively allometric relative to load arm estimates of the mandible (i.e., mandible length and the distance from the TMJ to the first molar). These findings suggest that, on the whole, larger-bodied primates are capable of generating larger muscle forces than their smaller-bodied counterparts, except in platyrrhines where large-bodied primates are at a relative disadvantage. These findings also suggest that patterns may vary considerably across taxonomic groups, likely in response to different functional demands, thus highlighting the importance of broad comparative analyses.

1.2. TMJ scaling

Only a handful of studies have addressed how specific aspects of the TMJ scale in relation to size (Smith et al., 1983; Bouvier, 1986a,b; Vinyard, 1999). Smith et al. (1983) examined condylar shape across female anthropoid primates and found that condylar dimensions (length, width, area) scale with slight positive allometry relative to body size. In contrast, s (1986a,b); s (1986a,b) analyses of condylar scaling in male Old and New World monkeys found that the same dimensions were largely isometric in relation to body size. More recently, Vinyard (1999) examined the scaling patterns of mandibular condyle and glenoid length, width, area, and aspects of joint curvature in strepsirrhines, and found that some dimensions (i.e., condyle width and area) scaled with positive allometry when regressed against mandible length and/or cranial size, though others (condyle length, glenoid length, and glenoid width) scaled with isometry.

The results of these prior analyses of the TMJ are somewhat conflicting, and to some extent the scope of these results is limited because the analyses examined only single components of the joint, rather than the entire joint complex. Notably, most of these analyses have been limited to the mandibular component of the TMJ, and very little attention has been paid to how the cranial component of the TMJ, the glenoid fossa, scales relative to cranial or body size (but see Vinyard, 1999). Importantly, there are many factors that may influence how the TMJ is loaded. Biomechanical models of the masticatory apparatus predict that the muscle resultant force must be equally opposed by the sum of the bite force and joint reaction forces. Muscle resultant force varies as a function of muscle firing patterns and the physiological cross-sectional area of the muscle, among other factors. Thus, all other factors being equal, absolute increases in muscle force will subsequently result in higher output forces (i.e., bite forces and/or joint reaction forces). Correspondingly, the distribution of these forces across both the bite force and the joint reaction force vary depending upon multiple factors, including the position of the bite point and the muscle resultant relative to the joint, the height of the TMJ above the occlusal plane, and the activity of the balancing vs. working side musculature (e.g., Hylander, 2006). TMJ scaling, however, is not only related to the loads experienced at the TMJ; we should also expect the features of the TMJ to vary in relation to the joint range of motion (Wall, 1995, 1999), either as a function of feeding behaviors or for other reasons such as social display behaviors or vocalizations. For example, analyses of TMJ form in primates that produce large gapes for feeding (i.e., tree-gouging primates) or canine displays (i.e., male *Macaca fascicularis*) indicate that these groups tend to have condyles that are more anteroposteriorly curved and TMJs that are located closer to the occlusal plane (Vinyard et al., 2003; Terhune et al., 2015). Thus, it is critical to consider multiple aspects of TMJ morphology that are related to the multiple performance variables important for TMJ function.

1.3. Methodological complications

It is likely that methodological differences are responsible for many of the conflicting results presented above. These include differences in scaling variables, taxonomic levels, sample composition and sex, and statistical approach.

There is significant debate regarding which independent variable(s) should be utilized in analyses of allometry. Smith (1993) defined two types of allometric analyses: body size allometry and biomechanical allometry. Body size allometry is concerned with the investigation of relationships between body size (as the explanatory variable) and a specific feature. This type of analysis is generally exploratory in nature and is “concerned with an underlying relationship that may be powerful, predictive, and founded on physical principles, but not well understood” (: p. 180). In contrast, biomechanical allometry is concerned with the study of patterns of relationships between two variables as size changes (Smith, 1993). In this type of analysis, the question of interest is not how variables change in size, but whether a relationship is maintained between two variables as size changes. Such analyses usually predict a specific slope given a biomechanical model relating two variables, neither of which represents overall size of the organism (Smith, 1993). As Hylander (1985) pointed out, the utility of body mass as the independent variable in analyses investigating the effects of size may be limited, particularly where the variables being analyzed are those that reflect the ability of the facial bones to resist stress, since the relationship between such variables is unlikely to be direct. As a result, in the masticatory biomechanics literature, mandible length (as an estimate of the bite force lever arm during incision) or the distance from the TMJ to the first molar (as an estimate of the bite force lever arm during mastication) have become the perhaps most frequently utilized scaling variables, rather than body mass (e.g., Hylander, 1985; Bouvier, 1986a,b; Ravosa, 1990, 1996, 2000; Vinyard, 1999, 2008; Taylor, 2002, 2005; Vinyard et al., 2003). The above-discussed studies are mixed in which variables they assess their measures of interest against, sometimes making it difficult to compare results among studies.

The above analyses naturally also vary in their sample composition, both in regard to the taxonomic groups included and in regard to the sexes of specimens analyzed. For example, Smith et al. (1983) examined only female anthropoid primates. Conversely, work by Bouvier

(1986a,b) focused solely on male cercopithecoids (Bouvier, 1986a) and male platyrrhines (Bouvier, 1986b), though she notes that similar patterns were obtained for females. In many cases (e.g., Ravosa, 1991; Vinyard, 1999; Vinyard and Hanna, 2005) females and males were pooled for analysis, rather than being analyzed separately (but see Daegling, 2001). This approach is problematic if one wishes to examine patterns that may be sexually dimorphic and/or assess how sexually dimorphic features such as canine size influence force versus gape production in the masticatory apparatus (e.g., Terhune et al., 2015).

Analytical methods also vary considerably across this previous research. In particular, there has been a shift in recent years toward the use of reduced major axis (RMA) regression and/or techniques that statistically control for phylogenetic covariance among samples (e.g., Felsenstein, 1985; Smith, 1993, 2009; Nunn and Barton, 2001; Freckleton et al., 2002; Blomberg et al., 2003). While ordinary least squares (OLS) regression is the more traditional approach, RMA regressions have been argued to be more appropriate in scaling analyses when the causality between the variables of interest is unknown and both variables are likely to contain error (Rayner, 1985; Smith, 1993, 2009; Sokal and Rohlf, 1995). Importantly, since RMA regressions are symmetric, the outcome of the regression analysis is not dependent upon which variable is placed on the X-axis, and as a result no causality of the relationship is implied. Both OLS and RMA regression techniques have recently been adapted to statistically account for phylogenetic covariance among data points. These phylogenetic regression techniques − phylogenetic generalized least squares (PGLS; Grafen, 1989) and phylogenetic reduced major axis (pRMA; Ives et al., 2007) − statistically control for non-independence of species data points by using a known (or assumed to be known) phylogeny to calculate expected covariance in the dataset. This expected covariance is then incorporated into the regression model as the error term (ε). However, with some exceptions (e.g., Vinyard and Hanna, 2005; Taylor et al., 2015), previous scaling analyses of the primate masticatory apparatus have not included controls for phylogenetic covariance among closely related taxa. Additionally, with the exception of Singleton (2005), most allometric studies of the masticatory apparatus have focused on the analysis of linear regressions of interlandmark distances using a bivariate allometric model. While geometric morphometric methods have been extensively employed to examine interspecific and ontogenetic allometry, this approach has not been applied in a biomechanical framework.

1.4. Scaling hypotheses

In addition to evaluating the general patterns of scaling in the TMJ, scaling patterns can also be used to test specific functional hypotheses. Three specific hypotheses regarding how aspects of the masticatory apparatus should scale based on physiological and/or biomechanical principles have been applied in previous studies (e.g., Anapol et al., 2008; Perry and Wall, 2008; Taylor et al., 2015) (Table 1).

1.4.1. Geometric similarity

Hypotheses of geometric similarity between body size and aspects of the TMJ, and/or mandible length and the TMJ assume that, as size increases, features of the TMJ scale with isometry. Identifying patterns of isometry would therefore suggest geometric (if not exactly functional) equivalence between small and large-bodied taxa. These hypotheses of isometry essentially serve as a null hypothesis. If isometry is rejected, then additional hypotheses can and should be evaluated.

1.4.2. Metabolic scaling

The metabolic scaling hypothesis, also known as Gould's scaling law (Gould, 1975), suggests that, since resting metabolic rate scales with the power of 0.75 relative to body mass (M_b) across mammals (e.g., Kleiber, 1932, 1947; Peters, 1983; Schmidt-Nielsen, 1984; McNab, 1988, 2003; Enquist et al., 2003; Savage et al., 2004; but see White and Seymour, 2003; White et al., 2009), postcanine occlusal area should also scale with a power of 0.75 (i.e., positive allometry, since the expected slope of isometry in this instance would be 0.67) so that animals can obtain the necessary amount of food per unit time. However, a number of subsequent analyses indicate that postcanine occlusal area in primates scales with isometry (e.g., Kay, 1975a,b; Fortelius, 1985; Vinyard and Hanna, 2005) rather than positive allometry. Further studies in mammals reveal a variety of dental scaling patterns across clades (Copes and Schwartz, 2010). Thus, alternate hypotheses for how primates and mammals meet their caloric needs have been proposed, including suggestions that larger animals spend relatively more time feeding, eat more energetically rich foods or extract energy more efficiently, and/or process more food per chew (Fortelius, 1985; Kay, 1985). For example, it has been suggested that daily ingested food volume scales with positive allometry (Ross et al., 2009a), which would result in larger-bodied primates spending more time feeding and chewing than smaller taxa.

Additionally, differences in the material properties of food items consumed may also be linked to variation in TMJ scaling patterns. Some authors interpret the positively allometric relationship between body size and mandibular dimensions in anthropoid primates (Hylander, 1985; Ravosa, 1996, 2000) as evidence for a size-related increase in dietary hardness and/or toughness (Kay, 1975a; Hylander, 1985; Sailer et al., 1985). In other words, these researchers suggest that smaller primate species tend to eat less resistant foods than larger species, which suggests that the magnitudes of forces generated and dissipated during mastication are larger in large-bodied taxa compared to small-bodied species. This could be linked to the increased reliance by larger primates on low-quality fallback foods, which tend to be more mechanically resistant (Marshall and Wrangham, 2007). If either of these relationships is valid (i.e., larger primates more frequently load their TMJs and/or produce higher magnitude loads), we would predict a positively allometric relationship between size and measures of TMJ shape that reflect load resistance.

1.4.3. Fracture scaling

Relative food object size is another critical factor when evaluating scaling patterns in the masticatory apparatus. The fracture scaling hypothesis (Lucas, 2004) suggests that large food particles fracture at lower stresses than smaller food particles, primarily as a result of how forces are distributed over the larger or smaller surface areas of these particles (i.e., stress = force/area). Assuming that these two food

Table 1
Expectations for each of the models discussed in this manuscript.

Model	Predictions[a]
Geometric similarity	Features of the masticatory apparatus will scale with **isometry** ($m = 1$)
Metabolic scaling	Features of the masticatory apparatus related to load resistance in the TMJ and/or mechanical advantage will scale with **positive allometry** ($m > 1$)
Fracture scaling	Features of the masticatory apparatus related to load resistance in the TMJ and/or mechanical advantage will scale with **negative allometry** ($m < 1$)
Food size scaling	Features of the masticatory apparatus related to jaw gape will scale with **negative allometry** ($m < 1$)

[a] So that all expected slopes (m) of isometry would be 1, I took the cube root of body mass and the square root of glenoid and condyle area prior to statistical analysis. Thus, my expectation for isometry for all regressions is $m = 1$.

Table 2
Samples included in this study with corresponding body mass data.

Taxon	Abbreviation	Sample size		Body mass[a] (g)		Museum
		Female	Male	Female	Male	
Alouatta belzebul	*Abel*	12	12	5520	7270	1
Alouatta palliata	*Apal*	12	12	5350	7150	1
Alouatta seniculus	*Asen*	12	12	5210	6690	1
Aotus trivirgatus	*Atri*	11	10	736	813	1
Ateles geoffroyi	*Ageo*	12	12	7290	7780	1
Cacajao melanocephalus	*Cmel*	8	14	2710	3160	1–3
Cebus albifrons	*Calb*	12	11	2290	3180	1
Cebus apella	*Cape*	11	12	2520	3650	1
Cebus capucinus	*Ccap*	13	11	2540	3680	1
Cercocebus torquatus	*Ctor*	4	5	6230	11000	1,3
Cercopithecus mitis	*Cmit*	12	12	4250	7930	4
Cercopithecus nictitans	*Cnic*	10	12	4260	6670	4
Chiropotes satanas	*Csat*	12	12	2580	2900	1,3
Colobus polykomos	*Cpol*	12	12	8300	9900	4
Erythrocebus patas	*Epat*	8	11	5770	10600	1,2,4
Gorilla beringei	*Gber*	8	10	97500	162500	1–4
Gorilla gorilla gorilla	*Ggor*	12	12	71500	170400	1,4
Homo sapiens[b]	*Hsap*	31	30	54425	62200	1
Hylobates agilis	*Hagi*	9	12	5820	5880	1,2
Hylobates klossii	*Hklo*	10	8	5920	5670	1,2
Hylobates lar	*Hlar*	10	12	5340	5900	1,3
Lagothrix lagotricha	*Llag*	11	12	7020	7280	1,2
Lophocebus albigena	*Lalb*	12	12	6020	8250	1,4
Macaca fascicularis	*Mfas*	12	12	3590	5360	1,5
Macaca fuscata	*Mfus*	12	9	8030	11000	1,2,5
Macaca nemestrina	*Mnem*	11	12	6500	11200	1–3,5
Macaca sylvanus	*Msyl*	9	4	11000	16000	1,2,5
Macaca thibetana	*Mthi*	3	7	9500	12200	1–3
Mandrillus sphinx	*Msph*	5	9	12900	31600	2,4,5
Miopithecus talapoin	*Mtal*	5	9	1120	1380	1,3–5
Nasalis larvatus	*Nlar*	12	12	9820	20400	1,5
Pan paniscus	*Ppan*	12	10	33200	45000	4
Pan troglodytes schweinfurthii	*Ptsch*	12	12	33700	42700	1–3
Pan troglodytes troglodytes	*Pttro*	7	9	45800	59700	1,2,4
Pan troglodytes verus	*Ptver*	4	5	44600	46300	1,2
Papio anubis	*Panu*	9	12	13300	25100	1,4
Papio cynocephalus	*Pcyn*	9	12	12300	21800	1,4,5
Papio ursinus	*Purs*	3	11	14800	29800	1,2,4,5
Piliocolobus badius	*Pbad*	12	12	8210	8360	1,4
Pithecia pithecia	*Ppit*	11	12	1580	1940	1–3
Pongo abelii	*Pabe*	9	10	35800	78500	1,5
Pongo pygmaeus	*Ppyg*	12	12	35600	77900	1,5
Procolobus verus	*Pver*	11	12	4200	4700	4
Saimiri sciureus	*Ssci*	10	10	668	779	1
Semnopithecus entellus	*Sent*	12	11	9890	13000	1,3,5
Symphalangus syndactylus	*Ssyn*	10	12	10700	11900	1,2,5
Theropithecus gelada	*Tgel*	3	10	11700	19000	1,2,3,5
Trachypithecus obscurus	*Tobs*	10	10	6260	7900	1,3

1 National Museum of Natural History, Washington, DC, USA; 2, American Museum of Natural History, New York, NY, USA; 3, Field Museum, Chicago, IL, USA; 4, Royal Museum for Central Africa, Tervuren, Belgium; 5, Department of Primatology at the State Collection of Anthropology and Paleoanatomy, Munich, Germany.

[a] Data from Smith and Jungers (1997).

[b] The sample of *H. sapiens* included here represents specimens from three populations of modern humans: Aleutian Islanders, Arikara from the Mobridge Site in South Dakota, and Late Woodland Bluff sample from Jersey County, Illinois.

particles have identical material properties, because of the increased surface area in the larger particle, less stress is required to fracture this particle than a smaller particle (Lucas, 2004). As a result, this relationship suggests that, if larger animals eat larger food items than smaller animals, larger animals will need to produce lower stresses to adequately process these foods. This would suggest that muscle PCSAs and/or mechanical advantage (i.e., the ratio between the muscle resultant and bite force) scales with negative allometry relative to body mass. However, only mixed support for this hypothesis has been found in analyses of muscle architecture (e.g., Anapol et al., 2008; Perry and Wall, 2008; Perry et al., 2011; Taylor et al., 2015). If the fracture scaling hypothesis is valid, we would predict a negatively allometric relationship between size and measures of TMJ shape that reflect load resistance.

1.4.4. Food size scaling

The metabolic scaling hypothesis as formulated by Gould (1975) assumes that the volume of food processed per chew scales isometrically with tooth surface area (Fortelius, 1985; Anapol et al., 2008), and the fracture scaling hypothesis assumes that food item size scales isometrically with body size (Lucas, 2004); neither of these assumptions may be valid. Although research by Perry and Hartstone-Rose (2010) found that maximum ingested food size scaled isometrically with body size and mandible length in strepsirrhines, subsequent work examining anthropoids (Perry et al., 2015) found a negatively allometric relationship between food size and body mass. Singleton (2005) suggests that, as body size increases, the percentage of foods that are relatively large in relation to body size should decrease. Thus, large gapes may be advantageous in taxa with relatively small body sizes so that large-diameter food items can be more easily processed and/or masticated. Since fewer food objects should present a mechanical challenge on the basis of food diameter for larger-bodied primates, relatively large gapes may not be maintained in taxa with increased body sizes, at least where there are no other selective pressures acting to maintain large gapes (e.g., large canine size). Accordingly, it would be expected that features of the TMJ related to generating large gapes (i.e., condylar and glenoid anteroposterior length, mandible length, TMJ height) scale with negative allometry relative to size. I refer to this model here as the food size scaling hypothesis. In taxa where there is strong selection for increased jaw gape (e.g., taxa with large canine sizes, gouging behaviors, or perhaps even some kinds of vocal behaviors) we could anticipate a departure from this scaling pattern.

1.5. Study goals

The goal of this study is to examine how scaling patterns in the masticatory apparatus, particularly the temporomandibular joint, inform our understanding of adaptation in the craniofacial skeleton of anthropoid primates. I will evaluate both the cranial and mandibular components of the TMJ, looking for general trends in scaling patterns both across anthropoids and between anthropoid clades, and I will test several explicit hypotheses generated from the biomechanical and feeding literature (see Table 1). As a null hypothesis, I will first test the prediction that the features of the TMJ scale with geometric equivalence (i.e., isometry).

Assuming that metabolic rate scales with positive allometry in relation to body mass (Gould, 1975), large-bodied primates must compensate for size-related increases in metabolic rate by obtaining more food per unit time than smaller primates. Compounded with the suggestion of a size-related increase in dietary resistance (Kay, 1975a; Hylander, 1985; Sailer et al., 1985), this suggests that larger primates must produce absolutely and/or relatively larger bite forces than small-bodied primates. In the TMJ, I would expect this to be manifested via positive allometry of features reflecting load resistance (e.g., condylar area), as higher bite forces (produced by absolutely larger bite forces,

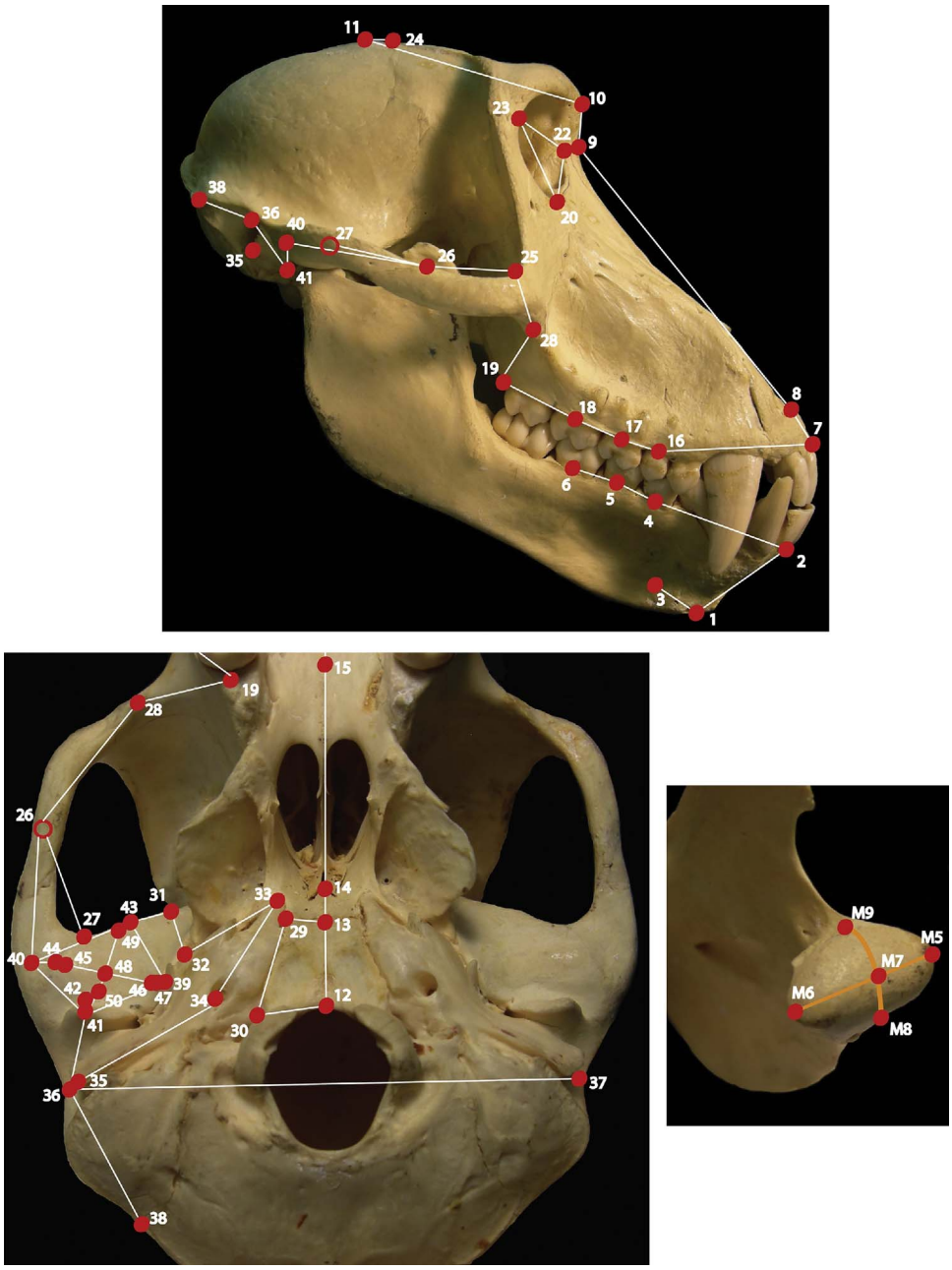

Fig. 1. Lateral view (top), inferior view (lower left) and mandibular condyle (lower right) of a *Papio anubis* cranium illustrating the landmarks used in this study. Lines on the mandibular condyle illustrate the mediolateral and anteroposterior axis of the joint used to identify the illustrated landmarks. Numbers correspond to landmarks defined in Table 3. Photographs not to scale.

and/or an increase in chew cycle duration/frequency [i.e., daily ingested food volume; Ross et al., 2009a,b]) would also likely result in higher cumulative joint reaction forces (i.e., summed forces generated either via increasing the magnitude of the force by eating more resistant foods and/or increasing the frequency of chewing). In this model, the magnitude of the bite force relative to the joint reaction force may still vary as a result of differences in mechanical advantage, but the overall forces are anticipated to be larger in large-bodied primates than in smaller primates, both absolutely and relatively. This model would also predict that larger-bodied primates would show positive allometry of features related to increased mechanical advantage (e.g., the lever-to-load arm ratio, height of the TMJ above the occlusal plane). Conversely, if the fracture scaling hypothesis is valid, then I would anticipate these same variables (i.e., those related to load resistance in the TMJ and/or mechanical advantage) to display negative allometry. Finally, if large gapes are more advantageous for small-bodied primates, then I anticipate observing a negatively allometric relationship between size and aspects of TMJ morphology related to gape behaviors.

I further examine patterns of allometry in craniofacial shape and glenoid shape across anthropoids by employing a geometric morphometric (GM) approach. Although patterns of positive or negative allometry cannot easily be assessed via geometric morphometrics, departures from isometry (which functions as the null hypothesis) can be examined. Importantly, this analysis also evaluates overall shape variation relative to a size variable, allowing covariation among features to be examined and compared among clades.

2. Materials and methods

Data included in this analysis were drawn from 1023 specimens from 46 species of anthropoid primates (including three subspecies of *Pan troglodytes* and three populations of modern *Homo sapiens*) (Table 2). Specimens included were all adult, as indicated by full eruption and occlusion of the third molar, and were free of pathologies.

Table 3
Landmarks used to extract the univariate variables and in the geometric morphometric analysis.

Landmark #	Description
1	Gnathion
2	Infradentale
3	Most inferior point on mental foramen
4	Point on lateral alveolar margin at the midpoint of mandibular P4
5	Point on lateral alveolar margin at the midpoint of mandibular M1
6	Point on lateral alveolar margin at the midpoint of mandibular M2
7	Prosthion
8	Nasospinale
9	Nasion
10	Glabella
11	Bregma
12	Basion
13	Midpoint of spheno-occipital synchondrosis
14	Hormion
15	Intersection of median and transverse palatine sutures
16	Point on alveolar margin at the midpoint of maxillary P4
17	Point on alveolar margin at the midpoint of maxillary M1
18	Point on alveolar margin at the midpoint of maxillary M2
19	Point just posterior to the alveolus of the last maxillary molar
20	Orbitale
21	Opposite side orbitale
22	Maxillofrontale
23	Frontomolare orbitale
24	Point where temporal line and coronal suture meet
25	Jugale
26	Point on the superior border of the zygomatico-temporal suture
27	Most posterior point on margin of temporal fossa in sagittal plane
28	Most anterior point on cranial masseteric scar
29	Most lateral point on anterior basicranium at the spheno-occipital synchondrosis
30	Most lateral point on posterior basicranium/most medial point on jugular fossa
31	Point at intersection of infratemporal crest and sphenotemporal suture
32	Most lateral point on foramen ovale
33	Apex of the petrous
34	Most inferolateral point on the carotid canal
35	Most inferior point on the tympanic plate/tube in the coronal plane of porion
36	Porion
37	Opposite side porion
38	Asterion
39[a]	Most inferior point on entoglenoid process
40[a]	Most inferior point on articular tubercle
41[a]	Most inferior point on postglenoid process
42[a]	Deepest point in mandibular fossa in sagittal plane of postglenoid point
43[a]	Most anterior point on the articular surface of the glenoid fossa
44[a]	Most lateral point on articular surface of glenoid at end of long axis of articular eminence
45[a]	Most lateral point on surface of articular eminence
46[a]	Most medial point on surface of articular eminence
47[a]	Most medial point on articular surface of glenoid at end of long axis of articular eminence
48[a]	Midpoint of crest of articular eminence
49[a]	Most anterior point on articular surface of glenoid along line perpendicular to the long axis of the articular eminence
50[a]	Point on posterior edge of articular eminence along line perpendicular to long axis of articular eminence
M1	Infradentale
M2	Midpoint of the occlusal surface of the central incisor
M3	Center of the occlusal surface of the ipsilateral mandibular third molar
M4	Center of the occlusal surface of the contralateral mandibular third molar
M5	Most lateral point on the articular surface of the mandibular condyle
M6	Most medial point on the articular surface of the mandibular condyle
M7	Midpoint of the line connecting the medial and lateral poles of the mandibular condyle
M8	Most posterior point on the articular surface of the mandibular condyle at the midpoint on the mediolateral curve
M9	Most anterior point on the mandibular condyle at the midpoint of the mediolateral curve

M1–M9 = landmarks not included in geometric morphometric analyses; note that infradentale was collected twice, once where the mandible was in occlusion with the cranium (landmark 2) and a second time when the mandible was removed from the cranium and digitized separately.
[a] Landmarks on glenoid fossa.

Species mean (and sex-specific) body mass data (Table 2) were taken from Smith and Jungers (1997). Data were collected using a Microscribe G2X digitizer (Immersion Corp., San Jose, CA, USA), with 59 landmarks total, 12 of which focused on the glenoid fossa (this configuration was used in the separate "glenoid only" geometric morphometric analyses), and 9 of which were collected separately on the mandible and were not included in the geometric morphometric analyses (Fig. 1 and Table 3).

2.1. Univariate data and analyses

These landmark data were used to extract 13 univariate measurements describing mandibular length, TMJ position above the occlusal plane, the size of several processes in the TMJ, as well as glenoid and condylar width, length, and area (Fig. 2 and Table 4). Mean values and standard deviations (SD) for these variables were calculated for each sex within a species (see Table S1 in the supplementary online Appendix).

The biomechanical significance of the variables analyzed here has been reviewed previously in Terhune (2010, 2011a, 2013). Briefly, these variables represent aspects of TMJ and masticatory shape that have been most closely connected to differences in load resistance and range of motion at the TMJ. Increased TMJ height above the occlusal plane has variably been linked to increased muscle attachment area, equalization of bite forces across the postcanine dentition, and increased length of the masseter and temporalis moment arms (Maynard Smith and Savage, 1959; Greaves, 1974, 1980; Herring and Herring, 1974; DuBrul, 1977; Ward and Molnar, 1980; Freeman, 1988; Spencer, 1995). Anteroposterior length of the glenoid and condyle have been related to variation in sagittal sliding at the TMJ (Wall, 1999; Vinyard et al., 2003). Increased glenoid length, measured here as both overall length of the glenoid and as an arc length along the articular eminence and preglenoid plane, suggests the capacity for increased translation of the condyle. Increased condylar length, measured here as both a chord and arc length, suggests increased capacity for rotation of the condyle. Similarly, increased overall glenoid area should more generally reflect increased range of motion at the joint. Though their exact roles are unclear, both the medially positioned entoglenoid process and the laterally placed articular tubercle have been suggested to guide condylar movements and to limit excessive mediolateral movements of the condyle during mastication (Greaves, 1978; Hylander, 1979; Wall, 1995, 1999; Sun et al., 2002). The biomechanical significance of the postglenoid process is perhaps even more enigmatic, but has primarily been suggested to limit posterior displacement of the mandibular condyle in the fossa (Sicher, 1951) and in some taxa may articulate with the mandibular condyle during mastication (Wall, 1997). Additionally, increased size of the processes surrounding the joint may act to increase joint congruence and therefore increase the area over which forces are distributed. Thus, the processes of the joint may play a role in both guiding condylar movements and/or decreasing stresses in the joint. Glenoid and condylar mediolateral width has been most closely related to resisting increased laterally focused stresses that are produced during twisting and lateral deviation of the mandible during mastication (Hylander, 1979; Hylander and Bays, 1979; Bouvier, 1986a,b; Taylor, 2005, 2006). Finally, increased surface area of the condyle functions to increase the area over which forces can be distributed, therefore decreasing stresses at the joint (Hylander, 1979; Smith

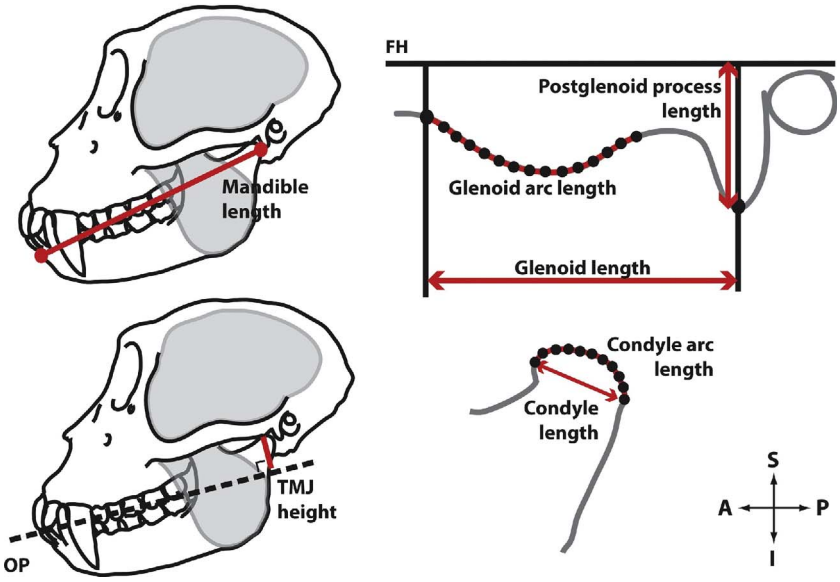

Fig. 2. Measurements collected in this study. Left: schematic of a *Macaca fascicularis* skull. Right: sagittal section through the glenoid fossa (top) and mandibular condyle (bottom). Measurements correspond to the definitions provided in Table 4. Not to scale. Abbreviations: FH, Frankfurt horizontal; OP, occlusal plane; A, anterior; I, inferior; P, posterior; S, superior.

Table 4
Definitions of univariate variables.

Variable name	Definition
Mandible length	Distance from the midpoint of the line connect the medial and lateral poles of the mandibular condyle to infradentale
TMJ height	Perpendicular distance from the midpoint of the line connecting the medial and lateral poles of the mandibular condyle to the mandibular occlusal plane[a]
Articular tubercle height	Distance from the most inferior point on the articular tubercle to Frankfurt horizontal[b]
Entoglenoid process height	Distance from the most inferior point on the entoglenoid process to Frankfurt horizontal[b]
Postglenoid process height	Distance from the most inferior point on the postglenoid process to Frankfurt horizontal[b]
Glenoid length	Distance from the most anterior point on the articular surface of the glenoid fossa to the most inferior point on the postglenoid process
Glenoid arc length	Sum of the distances between semilandmarks from the anteriormost attachment of the glenoid fossa joint capsule to the posterior edge of the articular eminence
Condyle length	Distance from the most anterior point on the articular surface of the mandibular condyle to the most posterior point on the articular surface of the mandibular condyle
Condyle arc length	Sum of the linear distances between semilandmarks from anterior to posterior on mandibular condyle articular surface at the midline
Glenoid width	Distance from the most inferior point on the entoglenoid process to the most inferior point on the articular tubercle
Condyle width	Distance from the most lateral point on the articular surface of the mandibular condyle to the most medial point on the articular surface of the mandibular condyle
Glenoid area	Three-dimensional surface area calculated from a point cloud covering the glenoid articular surface
Condyle area	Three-dimensional surface area calculated from a point cloud covering the condylar articular surface

[a] The occlusal plane was defined as the plane connecting the tip of the central incisor, the center of the occlusal surface of the left mandibular M3, and the center of the occlusal surface of the right mandibular M3.
[b] Frankfurt horizontal was defined as the plane connecting left orbitale, right orbitale, and porion (left or right).

et al., 1983; Bouvier, 1986a,b; Taylor, 2005).

Each of these variables was separately regressed on one of two independent variables representing size: body mass and mandible length. I included both of these variables here to examine how features of the TMJ scale relative to overall size of the organism (body mass), and a biomechanically relevant scaling variable (mandible length, which represents the lever arm during incision) (Hylander, 1985; Vinyard, 2008). Males and females were examined separately, and scaling patterns were assessed across the entire anthropoid sample and separately for each taxonomic subgroup (platyrrhines, cercopithecoids, and hominoids). All data were natural log (ln) transformed prior to analysis. So that all expected slopes (m) of isometry would be 1, I took the cube root of body mass and the square root of glenoid and condyle area prior to log transformation. Thus, my expectation for geometric similarity (i.e., isometry) for all regressions was $m = 1$ (see Table 1).

Following Smith (2009) and Ives et al. (2007) I employed phylogenetically corrected reduced major axis regression (pRMA) and performed a hypothesis test for departures from isometry ($H_0 = 1$). All bivariate regression analyses were conducted in R using the package *phytools* and the function phyl.RMA (Revell, 2012), where Pagel's lambda (λ) (Pagel, 1999; Freckleton et al., 2002) was optimized as part of the regression function. I calculated log-likelihood ratios to test whether λ was significantly different from 0 and/or 1; $\lambda = 0$ suggests no phylogenetic structure to the data, while $\lambda = 1$ is consistent with a Brownian motion model of evolution. Because I conducted a large number of analyses, I guarded against Type I error by performing a sequential Bonferroni adjustment (Rice, 1989) of the regression p-values (applied separately for each taxonomic group, dependent variables, and sex), and further differentiated between positive allometry − where the slope was > 1 and the p-value of the hypothesis test of isometry was $p < 0.00385$ (i.e., $\alpha = 0.05/13$) − and slight positive allometry − where the slope was > 1 and the p-value of the hypothesis test of isometry was $0.05 > p > 0.00385$. The consensus phylogeny used in the pRMA (and in the geometric morphometric analyses described below) was downloaded from http://10ktrees.nunn-lab.org (Arnold et al., 2010) (Fig. 3).

2.2. Geometric morphometric analyses

To assess overall scaling patterns in the cranium, masticatory apparatus, and TMJ, I performed a series of geometric morphometric analyses on two landmark configurations, one representing craniofacial

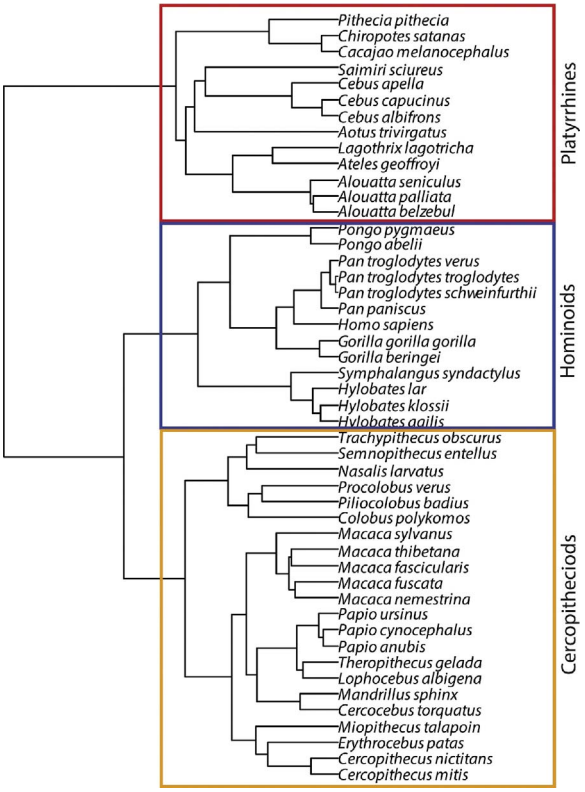

Fig. 3. Consensus phylogenetic tree with branch lengths (downloaded from http://10ktrees.nunn-lab.org; Arnold et al., 2010).

form (including the glenoid), and another representing just the glenoid fossa. Analyses were run separately for females and males so that differences due to sexual dimorphism could be examined, and datasets were subdivided taxonomically to look at scaling patterns separately in platyrrhines, cercopithecoids, and hominoids in addition to the entire anthropoid sample.

First, landmark configurations were superimposed using generalized Procrustes analysis (GPA). Then, the extent to which a phylogenetic signal was present in the dataset was assessed by calculating the sum of squared changes in shape along the branches of the consensus phylogeny; the significance of this relationship was calculated via a permutation test (9,999 iterations) where shape data were shuffled among the tips of the phylogenetic tree (Klingenberg, 2009). I employed a phylogenetic multivariate regression using the procD.pgls function in the R package *geomorph* (Adams and Otárola-Castillo, 2013), where the Procrustes-aligned coordinates ("shape") were regressed separately on the natural log of body mass and mandible length to examine how cranial shape varied in relation to overall body size and the biomechanical scaling variable. This function performs a phylogenetic ANOVA/regression and assumes a Brownian motion model of evolution. Data were permuted (9,999 iterations) across the tips of the phylogeny and compared to the original test statistic to determine significance of the regression relationship. To determine whether allometric trajectories for each clade (platyrrhines, cercopithecoids, hominoids) were significantly different from one another, the shape data for each clade were regressed on the size variable of interest and the angle between the vector trajectories was calculated. The significance of the angles was evaluated via a permutation test. Wireframe diagrams were employed to examine shape variation at the two ends of the regression plot. All analyses were conducted using the R package *geomorph* or the program MorphoJ (Klingenberg, 2009).

3. Results

3.1. Bivariate regressions

A summary of the bivariate regression results can be found in Table 5. Nearly all of the scaling relationships examined were statistically significant (Tables 5–9; supplementary Figs. S1–S4), with the exception of a handful of relationships for female hominoids relative to body mass (i.e., articular tubercle height, entoglenoid process height, postglenoid process height, glenoid arc length, and condyle arc length), a single variable (postglenoid process height) in male hominoids relative to body mass, and condyle arc length in female platyrrhines relative to mandible length. The lambda values indicating the strength of the phylogenetic relationships for each regression model were, with only a few exceptions, very high, many of which approached $\lambda = 1$ and/or were statistically indistinguishable from $\lambda = 1$. This was true for all regressions, regardless of taxonomic grouping, sex, or independent variable. The two scaling variables employed here largely scale with isometry relative to one another, though mandible length scales with slight positive allometry relative to body mass in cercopithecoids (Fig. 4).

Most relationships between aspects of TMJ shape or position relative to either body mass or mandible length were positively allometric or isometric (Table 5). TMJ height, articular tubercle height, entoglenoid process height, and postglenoid process height were most consistently positively allometric across taxonomic groupings, sex, and independent variable. Notably, TMJ height above the occlusal plane scaled with positive allometry in all analyses except male cercopithecoids (Fig. 5). Processes in the TMJ (articular tubercle height, entoglenoid height, and postglenoid height) all primarily scaled with positive allometry, though articular tubercle height was isometric relative to mass and mandible length in female platyrrhines and hominoids.

Features linked to increased translation at the joint (i.e., glenoid length and glenoid arc length) were primarily found to be isometric, with only one instance where slight positive allometry was identified (male platyrrhines vs. ln body mass), and in several cases were instead found to be negatively allometric (male and female cercopithecoids vs. mandible length and all taxa males vs. mandible length). However, features linked to more rotation at the TMJ (i.e., condyle length and condyle arc length) were more frequently positively allometric (though usually only slightly so). Measures of joint width showed a mixture of signals, with either isometry or positive allometry (but never negative allometry). Joint area measurements were primarily isometric, though notably condylar area scaled with negative allometry in male cercopithecoids relative to mandible length.

Scaling patterns varied across taxonomic groups, particularly for measures of anteroposterior condylar or glenoid fossa length, mediolateral width, and area. All relationships that were negatively allometric were relative to mandible length, and all were found in cercopithecoids, particularly male cercopithecoids. It is likely that this pattern in male cercopithecoids drove the finding of slight negative allometry of glenoid arc length relative to mandible length in the entire male sample. Hominoids (especially females) showed considerably more relationships that were not significant relative to body mass; this seems to be especially driven by the inclusion of the human sample, where humans tend to have small joint processes (i.e., the articular tubercle, entoglenoid process, and postglenoid process) relative to body mass, but less so relative to mandible length (though this is still true for postglenoid process height) (supplementary Figs. 1–4).

3.2. Geometric morphometric analyses

The geometric morphometric analyses expand on and extend the scaling analyses reviewed above. Regression of craniofacial shape on both body mass and mandible length (Table 10) revealed that craniofacial shape is

Table 5
Summary of allometric analyses. Boxes highlighted in gray represent relationships that are positively allometric, boxes that are outlined and bolded represent negatively allometric relationships.

		All Taxa		Platyrrhines		Cercopithecoids		Hominoids	
	Dependent	Female	Male	Female	Male	Female	Male	Female	Male
vs. Body mass	Mandible length	I	~+	I	I	~+	~+	I	I
	TMJ height	+	+	~+	~+	+	I	~+	~+
	Articular tubercle height	+	+	I	~+	+	+	NS	I
	Entoglenoid height	+	+	~+	+	+	+	NS	~+
	Postglenoid process height	+	+	~+	~+	+	+	NS	NS
	Glenoid length	I	I	I	I	I	I	I	I
	Glenoid arc length	I	I	I	~+	I	I	NS	I
	Condyle length	~+	~+	I	I	~+	I	I	I
	Condyle arc length	I	I	I	~+	I	I	NS	I
	Glenoid width	~+	~+	I	I	~+	I	I	I
	Condyle width	+	+	I	I	~+	I	I	I
	Glenoid area	~+	~+	I	I	I	I	I	I
	Condyle area	~+	I	I	I	I	I	I	I
vs. Mandible length	TMJ height	+	~+	+	~+	~+	I	+	~+
	Articular tubercle height	+	+	I	~+	~+	+	I	I
	Entoglenoid height	+	+	+	+	~+	+	~+	+
	Postglenoid process height	+	+	I	~+	~+	+	~+	~+
	Glenoid length	I	I	I	I	I/–	–	I	I
	Glenoid arc length	I	I/–	I	I	I	I/–	I	I
	Condyle length	~+	I	I	I	I	I	~+	~+
	Condyle arc length	I	I	NS	I	I	I	I	I
	Glenoid width	I	I	I	I	I	I	~+	+
	Condyle width	+	~+	I	I	I	I	~+	~+
	Glenoid area	I	I	I	I	I	I	I	I
	Condyle area	I	I	I	I	I	–	I	I

+ positive allometry.
~ + slight positive allometry (test for slope significance is 0.00385 (= 0.05/13) > but < 0.05).
I/– slope CI does not quite encompass 1, but significance of slope is > 0.05.
– negative allometry.
I, isometry.
NS, no significant relationship.

strongly allometric, and that cercopithecoids in particular show the strongest relationship between size and shape, with the male sample having higher R^2 values than the females. The relationship between size and shape is substantially tighter when shape is evaluated relative to mandible length rather than body mass. This is at least in part due to the fact that the body mass data were culled from the literature, whereas the mandible length data were taken from this specific sample. Analysis of the angles between trajectory vectors (Table 11) for the platyrrhine, cercopithecoid, and hominoid subsamples indicates that all three trajectories are significantly different from one another in morphospace at $p < 0.05$. This is true for both males and females and relative to both body mass and mandible length.

Patterns of craniofacial shape variation across the different body sizes are very similar for males and females and for both independent variables. In general, the male and female patterns are very similar, though the male sample shows a wider range of body sizes; for ease of illustration I focus here on results for the male sample (Figs. 6 and 7; female plots are shown in supplementary Figs. 5 and 6). In general, smaller taxa have TMJs relatively closer to the occlusal plane, more orthognathic faces, small temporalis muscles relative to their cranial size, small glenoid fossae, and more anteriorly positioned zygomatic arches (and therefore masseter muscles) that are closer to the postcanine tooth row. In contrast, large taxa have TMJs positioned well above the occlusal plane, considerably longer/more projecting faces, larger temporalis muscles, larger glenoid fossae relative to the overall size of the landmark configuration, and more posteriorly positioned zygomatic arches relative to the tooth row.

When the configuration of the glenoid fossa is examined in isolation from the rest of craniofacial shape, there are fewer significant relationships between size and glenoid shape (Table 10). Both platyrrhine males and females show a significant relationship between glenoid shape and body mass, but not between glenoid shape and mandible length. Only cercopithecoid males exhibit a significant relationship between glenoid shape relative to both body mass and mandible length. Comparison of regression trajectories also distinguishes cercopithecoids from hominoids, but not platyrrhines (Table 11). These results suggest that glenoid shape variation is less closely tied to overall size variation, and that differences among taxa are more subtle. At least when the entire anthropoid sample is examined, smaller taxa tend to have anteroposteriorly longer glenoid fossae, larger postglenoid processes, and flatter articular eminences. By comparison, larger taxa tend to have mediolaterally wider glenoid fossae, smaller postglenoid processes, more pronounced articular tubercles, and more raised articular eminences.

4. Discussion

How masticatory apparatus shape changes relative to size can inform our understanding of masticatory adaptation. In primates,

Table 6
Regression statistics for female univariate data regressed on the natural log of body mass (lnmass). λ = lambda values indicating strength of the phylogenetic relationship; R^2 = regression coefficients; CI = confidence interval; Slope_p = p-value representing the significance of the hypothesis test of isometry; significant p-values indicate departures from the expected slope of 1. Symbols explaining the allometric results can be found in Table 5.

vs. lnmass	FEMALES							
	λ[a]	R^2	p-value[b]	Intercept	Slope	Slope 95% CI	Slope_p[c]	Allometric result
Mandible length	0.97**	0.805	<0.0001	1.05	1.11	0.96–1.25	0.128	Isometry
Platyrrhines	1*	0.853	<0.0001	1.27	1.04	0.77–1.31	0.733	Isometry
Cercopithecoids	0.98*	0.870	<0.0001	0.75	1.20	1–1.41	0.035	~+
Hominoids	0.96*	0.590	0.002	1.10	1.06	0.61–1.51	0.767	Isometry
TMJ height	0.98**	0.687	<0.0001	−2.14	1.72	1.44–2.01	**<0.0001**	+
Platyrrhines	1*	0.653	0.001	−3.29	2.21	1.5–2.93	0.018	~+
Cercopithecoids	1*	0.700	<0.0001	−2.24	1.70	1.26–2.14	**0.0005**	+
Hominoids	0.95*	0.632	0.001	−2.13	1.68	1–2.36	0.017	~+
Articular tubercle height	0.97**	0.444	<0.0001	−2.81	1.59	1.23–1.94	**0.0002**	+
Platyrrhines	1*	0.396	0.021	−2.62	1.57	0.76–2.38	0.080	Isometry
Cercopithecoids	0.86*	0.556	<0.0001	−3.22	1.71	1.17–2.24	**0.002**	+
Hominoids	0.95*	0.165	0.169	−2.68	1.49	0.6–2.38	0.175	NS
Entoglenoid height	0.99*	0.484	<0.0001	−3.15	1.75	1.37–2.12	**<0.0001**	+
Platyrrhines	1*	0.687	0.0005	−3.12	1.77	1.11–2.44	0.007	~+
Cercopithecoids	1*	0.675	<0.0001	−2.56	1.51	1.1–1.91	0.005	+
Hominoids	0.98*	0.147	0.195	−4.26	2.06	0.81–3.3	0.023	NS
Postglenoid process height	0.99*	0.337	<0.0001	−3.17	1.81	1.37–2.24	**<0.0001**	+
Platyrrhines	1*	0.562	0.003	−2.31	1.58	0.88–2.27	0.044	~+
Cercopithecoids	0.3x	0.663	<0.0001	−2.50	1.58	1.15–2.01	**0.003**	+
Hominoids	0.99*	0.044	0.493	−4.71	2.11	0.76–3.46	0.025	NS
Glenoid length	0.95**	0.784	<0.0001	−0.46	1.10	0.95–1.25	0.173	Isometry
Platyrrhines	1*	0.832	<0.0001	−0.62	1.18	0.86–1.51	0.204	Isometry
Cercopithecoids	0.88*	0.862	<0.0001	−0.41	1.08	0.89–1.27	0.385	Isometry
Hominoids	0.92*	0.543	0.004	−0.68	1.14	0.63–1.65	0.533	Isometry
Glenoid arc length	0.96**	0.666	<0.0001	−0.64	1.04	0.86–1.23	0.629	Isometry
Platyrrhines	1*	0.600	0.005	−1.24	1.29	0.67–1.91	0.257	Isometry
Cercopithecoids	0.75*	0.850	<0.0001	−0.79	1.09	0.89–1.29	0.348	Isometry
Hominoids	0.96*	0.287	0.059	−0.40	0.95	0.42–1.47	0.832	NS
Platyrrhines	1*	0.382	0.043	−2.39	1.48	0.61–2.35	0.165	Isometry
Cercopithecoids	0.64**	0.505	0.0002	−1.09	1.00	0.67–1.33	0.988	Isometry
Hominoids	0.91**	0.332	0.039	−1.84	1.25	0.58–1.93	0.381	NS
Glenoid width	0.96**	0.789	<0.0001	−0.82	1.21	1.04–1.37	0.009	~+
Platyrrhines	1*	0.831	<0.0001	−0.28	1.03	0.74–1.31	0.832	Isometry
Cercopithecoids	0.64**	0.856	<0.0001	−0.95	1.23	1.01–1.46	0.025	~+
Hominoids	0.93*	0.669	0.001	−1.43	1.36	0.84–1.89	0.105	Isometry
Condyle width	0.95**	0.754	<0.0001	−1.42	1.33	1.13–1.52	**0.0004**	+
Platyrrhines	1*	0.809	<0.0001	−0.78	1.12	0.79–1.46	0.395	Isometry
Cercopithecoids	0.82*	0.811	<0.0001	−1.61	1.37	1.08–1.65	0.005	~+
Hominoids	0.9**	0.603	0.002	−2.19	1.52	0.88–2.16	0.051	Isometry
Glenoid area	0.97**	0.788	<0.0001	−0.72	1.17	1.01–1.34	0.028	~+
Platyrrhines	1*	0.569	0.007	−0.59	1.16	0.59–1.74	0.513	Isometry
Cercopithecoids	0.77*	0.849	<0.0001	−0.78	1.17	0.96–1.39	0.083	Isometry
Hominoids	0.93**	0.731	0.0002	−1.02	1.24	0.81–1.67	0.205	Isometry
Condyle area	0.94**	0.742	<0.0001	−1.17	1.18	0.99–1.36	0.042	~+
Platyrrhines	1*	0.546	0.009	−1.28	1.24	0.61–1.86	0.369	Isometry
Cercopithecoids	0.8*	0.834	<0.0001	−1.02	1.11	0.89–1.32	0.288	Isometry
Hominoids	0.89**	0.598	0.002	−1.65	1.30	0.75–1.86	0.194	Isometry

[a]* = Lambda significantly different from 0 but not from 1; ** = lambda significantly different from 0 and 1; + = lambda significantly different from 1 but not 0; x = lambda not significantly different from 0 or 1
[b]Highlighted cells are significant after sequential Bonferroni adjustment.
[c]Highlighted cells are significant at $p < 0.05$; bolded values are also significant at $p < 0.00385$ (= 0.05/13).

Table 7
Regression statistics for male univariate data regressed on the natural log of body mass (lnmass). λ = lambda values indicating strength of the phylogenetic relationship; R^2 = regression coefficients; CI = confidence interval; Slope_p = *p*-value representing the significance of the hypothesis test of isometry; significant *p*-values indicate departures from the expected slope of 1. Symbols explaining the allometric results can be found in Table 5.

vs. lnmass	MALES							
	λ[a]	R^2	*p*-value[b]	Intercept	Slope	Slope 95% CI	Slope_p[c]	Allometric result
Mandible length	0.98**	0.837	<0.0001	0.93	1.14	1.01–1.28	0.031	~+
Platyrrhines	1*	0.803	<0.0001	0.93	1.17	0.82–1.53	0.257	Isometry
Cercopithecoids	0.97*	0.912	<0.0001	0.71	1.22	1.05–1.39	0.009	~+
Hominoids	0.96*	0.686	0.0005	1.00	1.08	0.67–1.48	0.670	Isometry
TMJ height	0.97**	0.598	<0.0001	−1.62	1.55	1.24–1.87	**0.0003**	+
Platyrrhines	1*	0.713	0.001	−4.64	2.73	1.92–3.54	0.009	~+
Cercopithecoids	0.46x	0.629	<0.0001	−1.23	1.36	0.93–1.78	0.057	Isometry
Hominoids	0.89**	0.657	0.0008	−1.87	1.58	0.96–2.19	0.027	~+
Articular tubercle height	0.98**	0.570	<0.0001	−3.14	1.70	1.36–2.03	<0.0001	+
Platyrrhines	0.97*	0.446	0.013	−3.24	1.81	0.92–2.71	0.023	~+
Cercopithecoids	0.62*	0.657	<0.0001	−3.49	1.80	1.31–2.3	**0.0003**	+
Hominoids	0.97*	0.461	0.011	−1.85	1.22	0.63–1.82	0.382	Isometry
Entoglenoid height	0.98*	0.673	<0.0001	−3.35	1.80	1.49–2.1	<0.0001	+
Platyrrhines	1*	0.704	0.0003	−3.65	1.97	1.25–2.69	**0.002**	+
Cercopithecoids	0.79*	0.784	<0.0001	−3.15	1.70	1.33–2.07	**0.0001**	+
Hominoids	0.98*	0.432	0.015	−3.62	1.82	0.91–2.74	0.023	~+
Postglenoid process height	0.98*	0.501	<0.0001	−3.45	1.88	1.49–2.28	**<0.0001**	+
Platyrrhines	1*	0.551	0.004	−2.83	1.77	0.98–2.56	0.017	~+
Cercopithecoids	0.32+	0.741	<0.0001	−2.73	1.64	1.25–2.04	**0.0004**	+
Hominoids	0.99*	0.216	0.110	−4.81	2.11	0.88–3.34	0.016	NS
Glenoid length	0.98**	0.797	<0.0001	−0.46	1.10	0.95–1.25	0.163	Isometry
Platyrrhines	1*	0.795	<0.0001	−0.98	1.33	0.92–1.73	0.064	Isometry
Cercopithecoids	0.88*	0.870	<0.0001	−0.27	1.03	0.86–1.21	0.699	Isometry
Hominoids	0.96*	0.680	0.0005	−0.66	1.12	0.7–1.55	0.517	Isometry
Glenoid arc length	0.97**	0.710	<0.0001	−0.66	1.05	0.88–1.22	0.540	Isometry
Platyrrhines	1*	0.496	0.015	−2.54	1.76	0.82–2.71	0.039	~+
Cercopithecoids	0.85*	0.864	<0.0001	−0.74	1.06	0.88–1.25	0.462	Isometry
Hominoids	0.96*	0.474	0.009	−0.56	0.98	0.51–1.46	0.941	Isometry
Condyle length	0.96**	0.809	<0.0001	−2.06	1.22	1.06–1.38	0.004	~+
Platyrrhines	1*	0.791	<0.0001	−2.07	1.27	0.88–1.65	0.119	Isometry
Cercopithecoids	0.83*	0.843	<0.0001	−2.03	1.18	0.96–1.4	0.078	Isometry
Hominoids	0.92**	0.730	0.0002	−2.46	1.30	0.85–1.76	0.123	Isometry
Condyle arc length	0.98**	0.622	<0.0001	−1.48	1.15	0.94–1.37	0.136	Isometry
Platyrrhines	1*	0.480	0.018	−3.97	2.06	0.94–3.17	0.014	~+
Cercopithecoids	0.93*	0.643	<0.0001	−1.32	1.11	0.79–1.42	0.464	Isometry
Hominoids	0.94**	0.659	0.0008	−1.35	1.09	0.66–1.52	0.635	Isometry
Glenoid width	0.98**	0.796	<0.0001	−0.86	1.22	1.05–1.38	0.006	~+
Platyrrhines	1*	0.822	<0.0001	−0.45	1.10	0.79–1.42	0.463	Isometry
Cercopithecoids	0.58x	0.821	<0.0001	−0.87	1.21	0.97–1.45	0.063	Isometry
Hominoids	0.96*	0.753	0.0001	−1.33	1.31	0.87–1.75	0.102	Isometry
Condyle width	0.95**	0.795	<0.0001	−1.26	1.26	1.09–1.43	**0.002**	+
Platyrrhines	1*	0.725	0.0002	−1.32	1.32	0.85–1.78	0.111	Isometry
Cercopithecoids	0.73*	0.818	<0.0001	−1.20	1.22	0.97–1.46	0.055	Isometry
Hominoids	0.93**	0.730	0.0002	−1.71	1.35	0.88–1.82	0.084	Isometry
Glenoid area	0.98**	0.819	<0.0001	−0.63	1.14	0.99–1.29	0.046	~+
Platyrrhines	1*	0.543	0.010	−1.39	1.46	0.72–2.2	0.128	Isometry
Cercopithecoids	0.83*	0.868	<0.0001	−0.63	1.12	0.93–1.31	0.181	Isometry
Hominoids	0.95*	0.805	<0.0001	−0.89	1.18	0.83–1.53	0.247	Isometry
Condyle area	0.97**	0.795	<0.0001	−0.98	1.11	0.96–1.27	0.128	Isometry
Platyrrhines	1*	0.571	0.007	−2.27	1.60	0.81–2.39	0.060	Isometry
Cercopithecoids	0.77*	0.820	<0.0001	−0.84	1.06	0.84–1.27	0.573	Isometry
Hominoids	0.92**	0.833	<0.0001	−1.17	1.14	0.83–1.45	0.311	Isometry

[a]* = Lambda significantly different from 0 but not from 1; ** = lambda significantly different from 0 and 1; + = lambda significantly different from 1 but not 0; x = lambda not significantly different from 0 or 1

[b]Highlighted cells are significant after sequential Bonferroni adjustment.

[c]Highlighted cells are significant at $p < 0.05$; bolded values are also significant at $p < 0.00385$ (= 0.05/13).

previous analyses have primarily identified patterns of either isometry or positive allometry in aspects of mandibular and craniofacial shape (e.g., Smith, 1983; Hylander, 1985; Bouvier, 1986a,b; Ravosa, 1991; Vinyard and Ravosa, 1998; Daegling, 2001), and the same is true of analyses examining masticatory muscle architecture (Anapol et al., 2008; Perry and Wall, 2008; Taylor and Vinyard, 2013; Taylor et al., 2015). Although a handful of analyses have specifically evaluated scaling of the TMJ (1983; Bouvier, 1986a,b; Vinyard, 1999), results of these analyses have been somewhat contradictory. As a critical component of the masticatory apparatus, how the TMJ changes in relation to size across and within anthropoid primates can reveal how particular selective pressures may have influenced TMJ shape and therefore masticatory function.

4.1. Bivariate scaling patterns

In the present study I examined four general hypotheses that have been used to explain how aspects of masticatory morphology may scale relative to size: geometric similarity, metabolic scaling, fracture scaling, and what I have termed here food size scaling (Table 1). In particular, I differentiated between features of the TMJ related to load resistance/force generation (i.e., TMJ height above the occlusal plane, glenoid and condylar width, and condylar area) and those features more closely linked with range of motion at the joint (i.e., glenoid area, glenoid and condylar length and curvature). For the bivariate regression analyses, I specifically hypothesized that, if large-bodied primates must compensate for size-related increases in metabolic rate by obtaining more food per unit time than smaller primates, and/or larger primates are at a disadvantage because their food tends to be more resistant, then large-bodied primates will display positive allometry of features reflecting load resistance in the TMJ and/or mechanical advantage. Conversely, if the fracture scaling hypothesis is valid, I anticipated observing negatively allometric relationships between aspects of TMJ shape reflecting joint loading, and body mass and/or mandible length. Finally, I predicted that, if small-bodied primates must generate large gapes to process food items that are relatively large for their body or cranial size, then there should be a negatively allometric relationship between size and features of the masticatory apparatus related to jaw gape. Results of my analyses suggest that the null hypothesis of geometric similarity can be largely rejected, and although support for the metabolic scaling hypothesis is somewhat equivocal, there is virtually no support for the fracture scaling hypothesis or for the food size scaling hypothesis.

Glenoid and condylar width exhibit both patterns of isometry and positive allometry across different sexes and clades relative to body mass and mandible length. When all taxa are analyzed together, glenoid and condylar width scale with positive allometry relative to body mass, but this relationship is not observed when the sample is broken down by clade (except when only male cercopiths are analyzed). Furthermore, only condyle width scales with positive allometry relative to mandible length across anthropoids, though both glenoid and condyle width scale with positive allometry in hominoid females and males. This result would seem to suggest that there is little to no consistent pattern between body size and TMJ width, and/or that, if loading frequency does increase in larger primates due to increases in the number of chewing cycles per day, then loading frequency is not linked to the predicted increase in TMJ width (i.e., contra Bouvier, 1986a,b).

Height of the TMJ above the occlusal plane, which has been linked to increased length of the masseter and temporalis moment arms and increased muscle attachment area (Maynard Smith and Savage, 1959; Greaves, 1974, 1980; Herring and Herring, 1974; DuBrul, 1977; Ward and Molnar, 1980; Freeman, 1988; Spencer, 1995), showed the most consistently positively allometric pattern, except in male cercopithecoids where TMJ height scaled with isometry relative to both body mass and mandible length. This markedly different scaling pattern in male cercopiths may be related to selection for increased jaw gapes in relation to increased canine size and male/male competition (e.g., Plavcan et al., 1995; Hylander, 2013). One mechanism (among others) for increasing jaw gape is to decrease the distance between the TMJ and the occlusal plane, which functions to decrease stretching of the masseter muscle during wide jaw opening (Herring and Herring, 1974). This pattern of decreased TMJ height in taxa producing wide jaw gapes has been observed in tree-gouging primates (Vinyard et al., 2003), with taxa that actively gouge trees to stimulate the flow of exudates having relatively lower TMJs than closely related non-gouging species. Similarly, this pattern was also observed in an intraspecific comparison between female and male *M. fascicularis,* where males have significantly lower TMJs than females (Terhune et al., 2015). These results therefore suggest this pattern may hold true across male cercopithecoids relative to females, but this pattern is not observed in platyrrhines or hominoids.

Condylar area, as a measure of how stresses are dissipated in the joint, was observed to scale almost exclusively with isometry relative to both body mass and mandible length. Since larger condylar areas are expected to provide larger surface areas for resisting and dissipating joint reaction forces (Hylander, 1979; Smith et al., 1983; Bouvier, 1986a,b; Taylor, 2005), I anticipated that this morphology in particular would scale with positive allometry if larger primates need to produce more cumulative bite forces to meet their caloric needs. Contra to previous findings of positive allometry in mandibular dimensions (Smith, 1983; Hylander, 1985; Ravosa, 1991; Vinyard and Ravosa, 1998; Daegling, 2001), however, this finding of isometry in condylar area suggests that joint reaction forces may also scale with isometry relative to body mass. These results are consistent with findings of condylar area scaling with isometry relative to body mass and mandible length in both male Old World monkeys and male New World monkeys (Bouvier, 1986a,b), but counter to the results of Smith et al. (1983) who observed slight positive allometry in condylar area in female anthropoid primates.

There were two interesting exceptions to this general pattern of isometry of condylar area: (1) when all female samples were pooled and regressed on body mass, condylar area was positively allometric, and (2) when only male cercopithecoids were examined, condylar area scaled with negative allometry relative to mandible length. The former finding is therefore consistent with Smith et al.'s (1983) work and highlights the potential loss of information when only a single sex is examined, since different patterns were identified for females and males. The latter relationship is particularly interesting since it is one of only two relationships that were fully negatively allometric (i.e., not borderline isometry/negative allometry). Like TMJ height above the occlusal plane, this finding for male cercopithecoids could be interpreted as representing selection for increased jaw gapes at the expense of being able to generate high bite forces (Terhune et al., 2015), since, all other factors being equal, it is difficult to simultaneously maximize both of these performance variables. Thus, with lower occlusal forces relative to body mass or mandible length, we would anticipate correspondingly lower joint reaction forces at larger sizes, which ultimately is reflected in a smaller relative condylar articular area. However, experimental analyses of rhesus macaque (*M. mulatta*) bite forces have observed that occlusal forces scaled with isometry relative to facial length (Dechow and Carlson, 1990). Thus, at least in this species, male and female occlusal forces are similar relative to mandible length. One complicating factor is that mandible length in cercopithecoids (both sexes, but particularly in males) is positively allometric relative to body size. This relationship is further interpreted to be a consequence of selection for increased gape related to canine display behaviors in males (Hylander, 2013; Terhune et al., 2015). Thus, the observation of negative allometry of condylar area (as well as glenoid length) relative to mandible length may at least in part be related to choice of the scaling variable. Additional analyses examining masticatory force production across female and male cercopithecoids would be valuable for further evaluating this observed pattern.

Table 8
Regression statistics for female univariate data regressed on the natural log of mandible length (lnmandlg). λ = lambda values indicating strength of the phylogenetic relationship; R^2 = regression coefficients; CI = confidence interval; Slope_p = p-value representing the significance of the hypothesis test of isometry; significant p-values indicate departures from the expected slope of 1. Symbols explaining the allometric results can be found in Table 5.

vs. lnmandlg	FEMALES							
	λ[a]	R^2	p-value[b]	Intercept	Slope	Slope 95% CI	Slope_p[c]	Allometric result
TMJ height	1*	0.758	<0.0001	−3.67	1.53	1.31–1.76	**<0.0001**	+
Platyrrhines	1*	0.842	<0.0001	−6.31	2.20	1.73–2.67	**0.003**	+
Cercopithecoids	0.82*	0.694	<0.0001	−3.41	1.44	1.06–1.82	0.009	~+
Hominoids	1*	0.903	<0.0001	−3.85	1.58	1.25–1.91	**0.001**	+
Articular tubercle height	0.98*	0.674	<0.0001	−4.34	1.44	1.2–1.69	**0.0001**	+
Platyrrhines	1*	0.399	0.020	−4.54	1.51	0.73–2.28	0.106	Isometry
Cercopithecoids	0.94*	0.743	<0.0001	−4.41	1.44	1.1–1.79	0.005	~+
Hominoids	0.94*	0.681	0.00051	−4.16	1.39	0.86–1.91	0.082	Isometry
Entoglenoid height	0.99*	0.738	<0.0001	−4.84	1.58	1.34–1.83	**<0.0001**	+
Platyrrhines	0.96*	0.810	<0.0001	−5.30	1.71	1.21–2.21	**0.002**	+
Cercopithecoids	0.84*	0.865	<0.0001	−3.53	1.26	1.04–1.48	0.013	~+
Hominoids	1*	0.570	0.00286	−6.95	2.06	1.16–2.96	0.004	~+
Postglenoid process height	1*	0.620	<0.0001	−4.99	1.66	1.35–1.96	**<0.0001**	+
Platyrrhines	0.97*	0.618	0.001	−4.21	1.51	0.88–2.13	0.052	Isometry
Cercopithecoids	0.54x	0.790	<0.0001	−3.55	1.32	1.03–1.6	0.015	~+
Hominoids	1*	0.478	0.009	−7.53	2.13	1.11–3.15	0.005	~+
Glenoid length	0.98**	0.912	<0.0001	−1.51	1.00	0.91–1.08	0.923	Isometry
Platyrrhines	1*	0.888	<0.0001	−2.06	1.14	0.88–1.39	0.235	Isometry
Cercopithecoids	0.76*	0.939	<0.0001	−1.08	0.89	0.79–1	0.060	I/–
Hominoids	0.95*	0.908	<0.0001	−1.82	1.07	0.85–1.28	0.503	Isometry
Glenoid arc length	1*	0.819	<0.0001	−1.63	0.95	0.82–1.07	0.388	Isometry
Platyrrhines	0.98*	0.816	0.0001	−3.03	1.29	0.87–1.71	0.109	Isometry
Cercopithecoids	0.82*	0.872	<0.0001	−1.48	0.90	0.75–1.06	0.225	Isometry
Hominoids	1*	0.740	0.0002	−1.53	0.92	0.61–1.24	0.617	Isometry
Condyle length	0.94**	0.885	<0.0001	−3.24	1.12	1–1.23	0.036	~+
Platyrrhines	0.95*	0.822	<0.0001	−3.15	1.10	0.79–1.42	0.453	Isometry
Cercopithecoids	0.74*	0.904	<0.0001	−2.92	1.02	0.87–1.17	0.755	Isometry
Hominoids	0.83**	0.915	<0.0001	−3.90	1.26	1.01–1.51	0.025	~+
Condyle arc length	0.94**	0.534	<0.0001	−2.50	1.02	0.81–1.23	0.847	Isometry
Platyrrhines	0.89*	0.362	0.050	−4.41	1.47	0.6–2.35	0.176	NS
Cercopithecoids	0.47+	0.653	<0.0001	−1.64	0.82	0.59–1.04	0.139	Isometry
Hominoids	0.93**	0.509	0.006	−3.11	1.17	0.63–1.72	0.466	Isometry
Glenoid width	1*	0.857	<0.0001	−1.97	1.09	0.97–1.22	0.119	Isometry
Platyrrhines	1*	0.867	<0.0001	−1.53	0.99	0.74–1.23	0.905	Isometry
Cercopithecoids	0.75*	0.860	<0.0001	−1.69	1.02	0.84–1.2	0.850	Isometry
Hominoids	1*	0.906	<0.0001	−2.77	1.27	1.01–1.53	0.029	~+
Condyle width	0.97**	0.881	<0.0001	−2.71	1.21	1.08–1.33	**0.001**	+
Platyrrhines	1*	0.922	<0.0001	−2.16	1.08	0.88–1.28	0.384	Isometry
Cercopithecoids	0.91*	0.870	<0.0001	−2.49	1.14	0.95–1.34	0.121	Isometry
Hominoids	0.9**	0.902	<0.0001	−3.62	1.40	1.1–1.7	0.005	~+
Glenoid area	1*	0.910	<0.0001	−1.75	1.04	0.95–1.14	0.346	Isometry
Platyrrhines	1*	0.862	<0.0001	−2.17	1.16	0.83–1.48	0.276	Isometry
Cercopithecoids	0.7*	0.924	<0.0001	−1.51	0.97	0.84–1.1	0.646	Isometry
Hominoids	1*	0.943	<0.0001	−2.20	1.14	0.96–1.33	0.096	Isometry
Condyle area	0.95**	0.880	<0.0001	−2.23	1.05	0.94–1.16	0.351	Isometry
Platyrrhines	1*	0.702	0.001	−2.96	1.23	0.72–1.74	0.284	Isometry
Cercopithecoids	0.53+	0.936	<0.0001	−1.68	0.91	0.8–1.02	0.106	Isometry
Hominoids	0.87**	0.889	<0.0001	−2.85	1.20	0.93–1.47	0.106	Isometry

[a]* = Lambda significantly different from 0 but not from 1; ** = lambda significantly different from 0 and 1; + = lambda significantly different from 1 but not 0; x = lambda not significantly different from 0 or 1
[b]Highlighted cells are significant after sequential Bonferroni adjustment.
[c]Highlighted cells are significant at $p < 0.05$; bolded values are also significant at $p < 0.00385$ (= 0.05/13).

Finally, I predicted a negatively allometric relationship between body size and aspects of TMJ morphology related to gape behaviors. The best evidence in support of this hypothesis is the observation that glenoid length and glenoid arc length scale with negative allometry relative to mandible length in cercopithecoids. This finding suggests that, as cercopithecoids (particularly male cercopiths) get larger, the anteroposterior length of the glenoid increases at a slower rate than anticipated for isometry. Thus, the distance over which the mandibular condyle is able to translate during wide jaw gapes is proportionately smaller with longer mandible lengths. This finding is particularly interesting as it is contra to the suggestion above that male cercopithecoids are under selection for increased jaw gape, since one way in which increased jaw gape could be facilitated is by increasing the relative length of the glenoid articular surface (Terhune et al., 2015). Again, however, the positively allometric relationship between mandible length (itself a target of selection for increased gape) and body mass may in part be driving this relationship. Notably, a similar pattern was not observed for condylar length (measured either as an arc or a chord length), where a number of the scaling relationships with either body mass or mandible length were found to be positively allometric. Instead, both condylar arc length and glenoid arc length were observed to scale with positive allometry in male platyrrhines when measured relative to body mass. One possible explanation for this pattern may be related to the distinctive howling behaviors observed in the largest-bodied platyrrhine, *Alouatta* (e.g., Carpenter, 1934; Hershkovitz, 1949; Altmann, 1959). Although maximum gape has not been directly measured in these primates, their vocal behaviors may necessitate relatively wide gapes, which is in turn reflected in these anteroposteriorly elongated dimensions of the TMJ (Terhune, 2011b).

Although the function of the various processes in the joint (i.e., articular tubercle, entoglenoid, and postglenoid process) is not well known, these processes have been suggested (Greaves, 1978; Hylander, 1979; Wall, 1995, 1997,1999; Sun et al., 2002) to limit excessive movements of the mandibular condyle, and therefore may perform important functions related to range of motion at the joint. Alternatively, enlargement of the articular tubercle and the entoglenoid process (though not the postglenoid process) may increase the area over which the condyle comes into contact with the glenoid fossa, therefore functioning to decrease stresses at the joint. Almost uniformly across all regression analyses examining any one of these processes, the observed relationship was positively allometric, relative to both mandible length and body mass. Unfortunately, this finding does little to elucidate the function of these processes and further work examining joint kinematics and the role of these processes in restricting condylar movements needs to be undertaken. Additionally, analyses examining congruence of the glenoid fossa and condyle may reveal how consistently these processes may be in contact with the condyle during mandibular movements.

4.2. Geometric morphometric scaling patterns

The results of the geometric morphometric analyses are broadly similar to those of the bivariate regressions, though they highlight some important patterns of covariation among particular features and reveal distinct scaling patterns in the separate clades of primates examined. Not surprisingly, results indicate the overall craniofacial form is tightly linked to both body mass and mandibular length. However, this is less true of glenoid fossa shape, where fewer significant relationships were observed. Across the entire sample, smaller primates have considerably smaller, less prognathic faces relative to overall cranial size, TMJs located closer to the occlusal plane, smaller and anteroposteriorly elongated glenoid fossae, and zygomatic arches (and thus origin of the masseter muscle) that are more anteriorly positioned relative to the postcanine dentition. In contrast, larger primates are considerably more prognathic, have TMJs located well above the occlusal plane, possess large and mediolaterally wide glenoid fossae relative to overall cranial size, and have zygomatic arches that are positioned more posterior to the postcanine dentition.

These scaling patterns have implications for biomechanical function of the masticatory apparatus across primates. Assuming that muscle architecture and input patterns are similar across body sizes (though they most certainly are not; e.g., Anapol et al., 2008; Taylor and Vinyard, 2013; Taylor et al., 2015), the masticatory apparatus of smaller-bodied primates would appear to be more favorably structured for increased mechanical advantage (i.e., the ratio of the muscle moment arm to the bite force moment arm). However, TMJs relatively closer to the occlusal plane may limit some of this mechanical advantage (e.g., Greaves, 1980; Spencer, 1995). By comparison, larger-bodied primates with their long mandibles and very prognathic faces seem to be at a relative disadvantage for generating high occlusal forces, though they compensate for this to some extent by increasing the height of the TMJ above the occlusal plane. Differences in glenoid fossa size may perhaps reflect these differences in mechanical advantage. For example, the more favorable mechanical advantage in smaller primates may allow these primates to convert more of their input muscle force to bite force (i.e., a better lever-to-load arm ratio), thus minimizing joint reaction forces. Conversely, larger-bodied primates may experience higher joint reaction forces than would be anticipated for their body size given their less favorable mechanical advantage. Relatively larger glenoid areas may therefore reflect these higher forces. Further evaluation of these and similar data is warranted to more clearly examine how mechanical advantage varies in relation to primate body size.

Slightly different patterns of allometric shape variation were observed in platyrrhines, cercopithecoids, and hominoids. The multivariate regressions that explained the most shape variation were found in cercopithecoids (especially males), suggesting a tighter relationship between overall craniofacial/glenoid shape and either body mass or mandible length. Interestingly, the pattern of shape changes with size in platyrrhines and hominoids differs substantially (Fig. 8), with somewhat opposite size-related shape changes from small to large-bodied taxa. In particular, the overall dimensions of the glenoid vary such that in platyrrhines, the glenoid is mediolaterally wide and anteroposteriorly short in small-bodied taxa, and gradually becomes both anteroposteriorly long and mediolaterally narrow in larger species. In hominoids this is reversed. One possible interpretation of these data is convergence between large-bodied atelines (i.e., *Alouatta*) and the small-bodied hylobatids. Both of these groups are noted for their unique vocal behaviors, and although no analyses have quantified gape during vocalization in these taxa, it could be hypothesized that these vocal behaviors should necessitate relatively larger gapes. Gape data recently collected by Hylander (2013) indicate that gibbons and siamangs do indeed have large gapes relative to their jaw lengths, although the few data points currently available for *Alouatta* may suggest relatively smaller gapes in this genus (Hylander, personal communication). However, mandibular and canine morphology differs radically between *Alouatta* and hylobatids, with the TMJ raised well above the occlusal plane in howlers, while the TMJ is positioned very close to the occlusal plane in gibbons and siamangs. As a result, even given the same amount of condylar translation in these two groups, hylobatids would attain greater relative gapes than *Alouatta*, simply by virtue of their mandibular configuration (Herring and Herring, 1974; Singleton, 2005). This substantial difference in mandibular morphology is likely a consequence of the radical reorganization of the cranial base in *Alouatta*, as associated with the enlargement of the vocal apparatus (Hershkovitz, 1949; Hill, 1962). A number of features of the cranial base and masticatory apparatus have been previously linked to the highly autapomorphic vocal apparatus in this genus, including a small cranial capacity, decreased cranial flexion, increased bigonial breadth, a deep mandibular corpus with an enlarged and rounded gonial angle, and a TMJ raised above the occlusal plane (Watanabe, 1982; Anapol and Lee, 1994). Among these, several characters can also be interpreted as providing increased mechanical advantage for the mastication of tough

Table 9
Regression statistics for male univariate data regressed on the natural log of mandible length (lnmandlg). λ = lambda values indicating strength of the phylogenetic relationship; R^2 = regression coefficients; CI = confidence interval; Slope_p = *p*-value representing the significance of the hypothesis test of isometry; significant *p*-values indicate departures from the expected slope of 1. Symbols explaining the allometric results can be found in Table 5.

vs. lnmandlg	MALES							
	λ[a]	R^2	*p*-value[b]	Intercept	Slope	Slope 95% CI	Slope_p[c]	Allometric result
TMJ height	0.99*	0.651	<0.0001	−2.80	1.34	1.08–1.59	0.007	~+
Platyrrhines	0.93*	0.859	<0.0001	−4.87	1.87	1.38–2.35	0.020	~+
Cercopithecoids	0.41x	0.649	<0.0001	−1.88	1.08	0.75–1.41	0.609	Isometry
Hominoids	0.88**	0.878	<0.0001	−3.31	1.46	1.11–1.8	0.005	~+
Articular tubercle height	0.96*	0.737	<0.0001	−4.45	1.47	1.24–1.69	**<0.0001**	+
Platyrrhines	0.78*	0.655	0.0008	−4.49	1.49	0.91–2.08	0.046	~+
Cercopithecoids	0.56x	0.795	<0.0001	−4.50	1.47	1.15–1.78	**0.002**	+
Hominoids	1*	0.739	0.0002	−3.02	1.14	0.75–1.53	0.411	Isometry
Entoglenoid height	1*	0.852	<0.0001	−4.84	1.58	1.39–1.76	**<0.0001**	+
Platyrrhines	0.82*	0.894	<0.0001	−5.38	1.72	1.34–2.1	**0.0003**	+
Cercopithecoids	0.58*	0.911	<0.0001	−4.11	1.39	1.19–1.58	**0.0002**	+
Hominoids	1*	0.814	<0.0001	−5.51	1.73	1.23–2.24	**0.002**	+
Postglenoid process height	0.96*	0.738	<0.0001	−4.85	1.62	1.37–1.86	**<0.0001**	+
Platyrrhines	0.86*	0.770	0.0001	−4.26	1.51	1.02–2	0.017	~+
Cercopithecoids	0.54+	0.848	<0.0001	−3.86	1.38	1.13–1.64	**0.002**	+
Hominoids	1*	0.572	0.003	−7.13	2.03	1.15–2.92	0.004	~+
Glenoid length	1*	0.920	<0.0001	−1.33	0.96	0.87–1.04	0.284	I
Platyrrhines	1*	0.911	<0.0001	−2.04	1.13	0.9–1.36	0.201	Isometry
Cercopithecoids	0.64**	0.951	<0.0001	−0.91	0.86	0.77–0.95	0.006	–
Hominoids	1*	0.939	<0.0001	−1.70	1.04	0.87–1.21	0.600	Isometry
Glenoid arc length	0.9**	0.875	<0.0001	−1.42	0.90	0.8–1	0.053	I/–
Platyrrhines	1*	0.928	<0.0001	−2.56	1.18	0.94–1.42	0.101	Isometry
Cercopithecoids	0.67*	0.923	<0.0001	−1.40	0.88	0.77–1	0.061	I/–
Hominoids	1*	0.627	0.001	−1.57	0.93	0.55–1.31	0.713	Isometry
Condyle length	0.97**	0.907	<0.0001	−3.07	1.07	0.97–1.17	0.148	Isometry
Platyrrhines	1*	0.814	<0.0001	−3.07	1.08	0.76–1.39	0.580	Isometry
Cercopithecoids	0.69*	0.941	<0.0001	−2.74	0.97	0.86–1.09	0.641	Isometry
Hominoids	0.9*	0.939	<0.0001	−3.64	1.20	1–1.4	0.035	~+
Condyle arc length	0.99*	0.654	<0.0001	−2.33	0.99	0.81–1.17	0.898	Isometry
Platyrrhines	0.97*	0.476	0.019	−4.14	1.41	0.64–2.18	0.187	Isometry
Cercopithecoids	0.81*	0.800	<0.0001	−1.96	0.91	0.71–1.1	0.340	Isometry
Hominoids	1*	0.422	0.016	−2.30	1.00	0.49–1.5	0.988	Isometry
Glenoid width	1*	0.902	<0.0001	−1.86	1.07	0.97–1.17	0.168	Isometry
Platyrrhines	1*	0.888	<0.0001	−1.32	0.94	0.73–1.15	0.543	Isometry
Cercopithecoids	0.74*	0.889	<0.0001	−1.63	1.00	0.84–1.16	0.971	Isometry
Hominoids	1*	0.975	<0.0001	−2.52	1.21	1.08–1.34	**0.003**	+
Condyle width	0.99*	0.906	<0.0001	−2.34	1.11	1.01–1.21	0.026	~+
Platyrrhines	1*	0.903	<0.0001	−2.37	1.12	0.89–1.36	0.249	Isometry
Cercopithecoids	0.76*	0.906	<0.0001	−1.95	1.01	0.86–1.15	0.917	Isometry
Hominoids	0.97*	0.941	<0.0001	−2.93	1.25	1.04–1.45	0.014	~+
Glenoid area	1*	0.924	<0.0001	−1.48	0.98	0.9–1.06	0.653	Isometry
Platyrrhines	0.95*	0.897	<0.0001	−1.52	1.00	0.76–1.25	0.992	Isometry
Cercopithecoids	0.78*	0.938	<0.0001	−1.31	0.93	0.82–1.04	0.189	Isometry
Hominoids	1*	0.942	<0.0001	−1.97	1.09	0.91–1.27	0.267	Isometry
Condyle area	1*	0.884	<0.0001	−1.80	0.95	0.85–1.05	0.358	Isometry
Platyrrhines	1*	0.793	0.0002	−2.29	1.07	0.7–1.44	0.669	Isometry
Cercopithecoids	0.55+	0.930	<0.0001	−1.46	0.87	0.76–0.98	0.028	–
Hominoids	1*	0.873	<0.0001	−2.07	1.02	0.78–1.27	0.827	Isometry

[a]* = Lambda significantly different from 0 but not from 1; ** = lambda significantly different from 0 and 1; + = lambda significantly different from 1 but not 0; x = lambda not significantly different from 0 or 1
[b]Highlighted cells are significant after sequential Bonferroni adjustment.
[c]Highlighted cells are significant at $p < 0.05$; bolded values are also significant at $p < 0.00385$ (= 0.05/13).

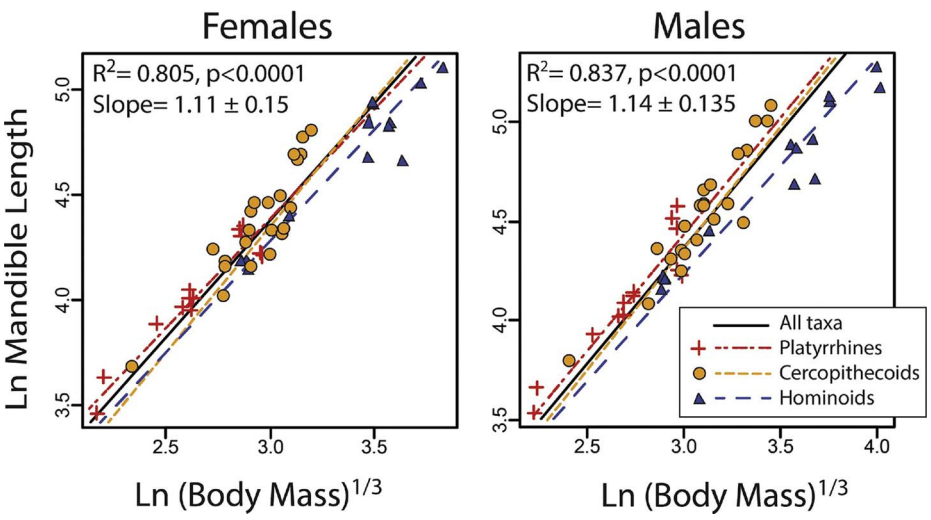

Fig. 4. Bivariate regressions of ln mandible length (y-axis) vs. ln body mass (x-axis) for females (left) and males (right). Regression statistics shown are for the entire pooled sample; regression statistics for individual clades can be found in Tables 6 and 8.

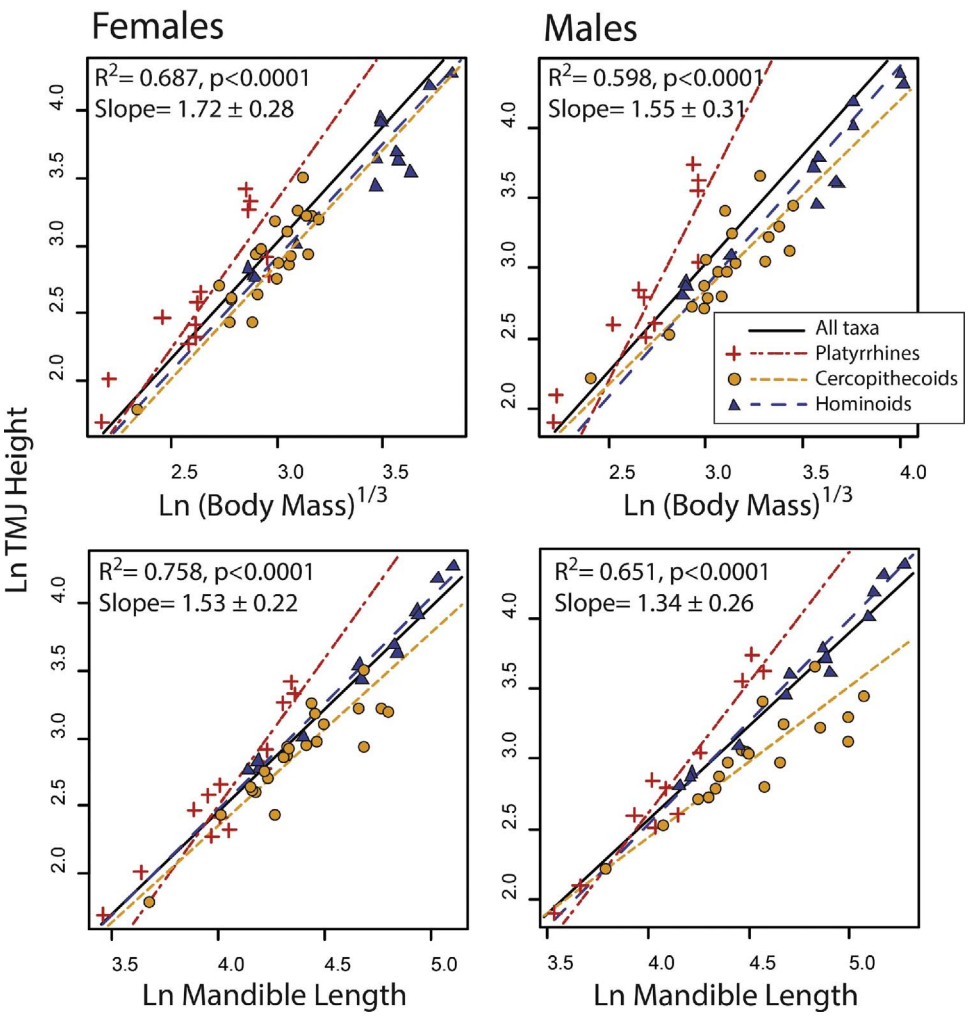

Fig. 5. Bivariate regressions of ln TMJ height (y-axis) vs. ln body mass (x-axis; top) and ln mandible length (bottom) for females (left) and males (right). Regression statistics shown are for the entire pooled sample; regression statistics for individual subsamples can be found in Tables 6–9.

food objects such as leaves, which *Alouatta* frequently relies on. In particular, the raised TMJ of *Alouatta* can be interpreted as acting to maximize the dispersion of bite forces along the postcanine dentition (Greaves, 1974, 1980; Spencer, 1995).

4.3. Outstanding questions and conclusions

A number of analyses (e.g., Kay, 1975a,b; Smith, 1983; Smith et al., 1983; Hylander, 1985; Bouvier, 1986a,b; Ravosa, 1991, 1996, 2000; Vinyard and Ravosa, 1998; Daegling, 2001; Vinyard and Hanna, 2005; Anapol et al., 2008; Perry and Wall, 2008; Copes and Schwartz, 2010; Taylor et al., 2015) have examined scaling patterns in the masticatory apparatus of primates, often with conflicting results. Given the variety of methodologies and samples employed in these analyses, the contradictory nature of some of these results is not especially surprising. Despite this, however, the overarching pattern across all of these

Table 10
Results of the multivariate regressions of the geometric morphometric data on body mass and mandible length. Highlighted cells are significant at $p < 0.05$; bolded values are also significant after sequential Bonferroni correction.

		vs. Body mass			vs. Mandible length		
		Platyrrhine	Cercopithecoid	Hominoid	Platyrrhine	Cercopithecoid	Hominoid
Cranium	Platyrrhine		49.6	76.9		55.9	65.4
			p < 0.00001	**p = 0.0032**		**p < 0.00001**	**p < 0.00001**
	Cercopithecoid	51.4		50.2	54.1		41.3
		p < 0.00001		**p < 0.00001**	**p < 0.00001**		**p < 0.00001**
	Hominoid	64.2	42.0		53.5	38.1	
		p < 0.00001	**p < 0.00001**		**p < 0.00001**	**p < 0.00001**	
Glenoid fossa	Platyrrhine		117.8	114.0		111.0	114.4
			p = 0.995	p=0.99		p = 0.97	p = 0.99
	Cercopithecoid	99.4		57.1	99.2		62.3
		p = 0.81		**p = 0.001**	p = 0.80		**p = 0.005**
	Hominoid	112.4	58.6		113.6	67.2	
		p = 0.98	**p = 0.002**		p = 0.99	**p = 0.02**	

Table 11
Angles (in degrees) between allometric trajectories and corresponding p-values. Significant *p*-values ($p < 0.05$) are highlighted in bold script.

		vs. Body mass			vs. Mandible length		
		Platyrrhine	Cercopithecoid	Hominoid	Platyrrhine	Cercopithecoid	Hominoid
Cranium	**Platyrrhine**		49.6	76.9		55.9	65.4
			p < 0.00001	**p = 0.0032**		**p < 0.00001**	**p < 0.00001**
	Cercopithecoid	51.4		50.2	54.1		41.3
		p < 0.00001		**p < 0.00001**	**p < 0.00001**		**p < 0.00001**
	Hominoid	64.2	42.0		53.5	38.1	
		p < 0.00001	**p < 0.00001**		**p < 0.00001**	**p < 0.00001**	
Glenoid fossa	Platyrrhine		117.8	114.0		111.0	114.4
			p = 0.995	p = 0.99		p = 0.97	p = 0.99
	Cercopithecoid	99.4		57.1	99.2		62.3
		p = 0.81		**p = 0.001**	p = 0.80		**p = 0.005**
	Hominoid	112.4	58.6		113.6	67.2	
		p = 0.98	**p = 0.002**		p = 0.99	**p = 0.02**	

analyses, including the work presented here, is one of isometric change in dimensions of the masticatory apparatus with size, and/or positive allometry in masticatory dimensions. That these dimensions do not overwhelmingly show positive allometry, as would be expected if masticatory dimensions scale at the same rate as metabolic rates scale relative to body mass (i.e., Gould, 1975), suggests that primates likely utilize some other mechanism(s) to meet their caloric needs. Another explanation may be related to more recent analyses of basal metabolic rate scaling that cast doubt on the conclusion that metabolism scales at a power of 0.75 to body mass and that the relationship between metabolism and body size may vary across taxonomic groups (e.g., White and Seymour, 2003; White et al., 2009). Notably, the research presented here emphasizes that patterns of allometry may vary considerably among clades and between sexes; thus it is likely that the mechanisms employed by primates to meet their daily metabolic needs vary widely and that there are likely to be multiple selective pressures acting on the masticatory apparatus in any given clade. These competing selective pressures are exemplified here in the cercopithecoid sample, where there is a clear signal, especially in males, that the need to increase gape in relation to increased canine size and social displays may adversely impact the mechanical advantage of the masticatory apparatus (e.g., Plavcan et al., 1995; Hylander, 2013; Terhune et al., 2015).

Perhaps the biggest challenge that comes with broad interspecific comparative analyses, such as the one presented here, is the lack of experimental data detailing variation in these performance variables. How bite force and range of motion scale relative to body mass and/or dimensions of the cranium (e.g., mandible length) is largely unclear, though some data in this regard are beginning to become available (e.g., Hylander, 2013). Similarly, observational data regarding how primates are actively using their masticatory apparatus is increasingly being collected in detail, as are the material properties of the foods being ingested by these species (e.g., Williams et al., 2005; Wright, 2005; Taylor et al., 2008; Vogel et al., 2008; Norconk et al., 2009; Ross et al., 2009a,b; McGraw et al., 2011, 2014). Ultimately it will only be through studies combining different lines of evidence – performance data, morphology (both as univariate measures of shape but also via geometric morphometric analyses), behavioral observations – that we will be able to come to more robust conclusions regarding the ways in which primates meet their caloric needs in the face of a wide range of selective pressures (e.g., Vinyard et al., 2011; Ross and Iriarte-Diaz, 2014; McNulty and Vinyard, 2015).

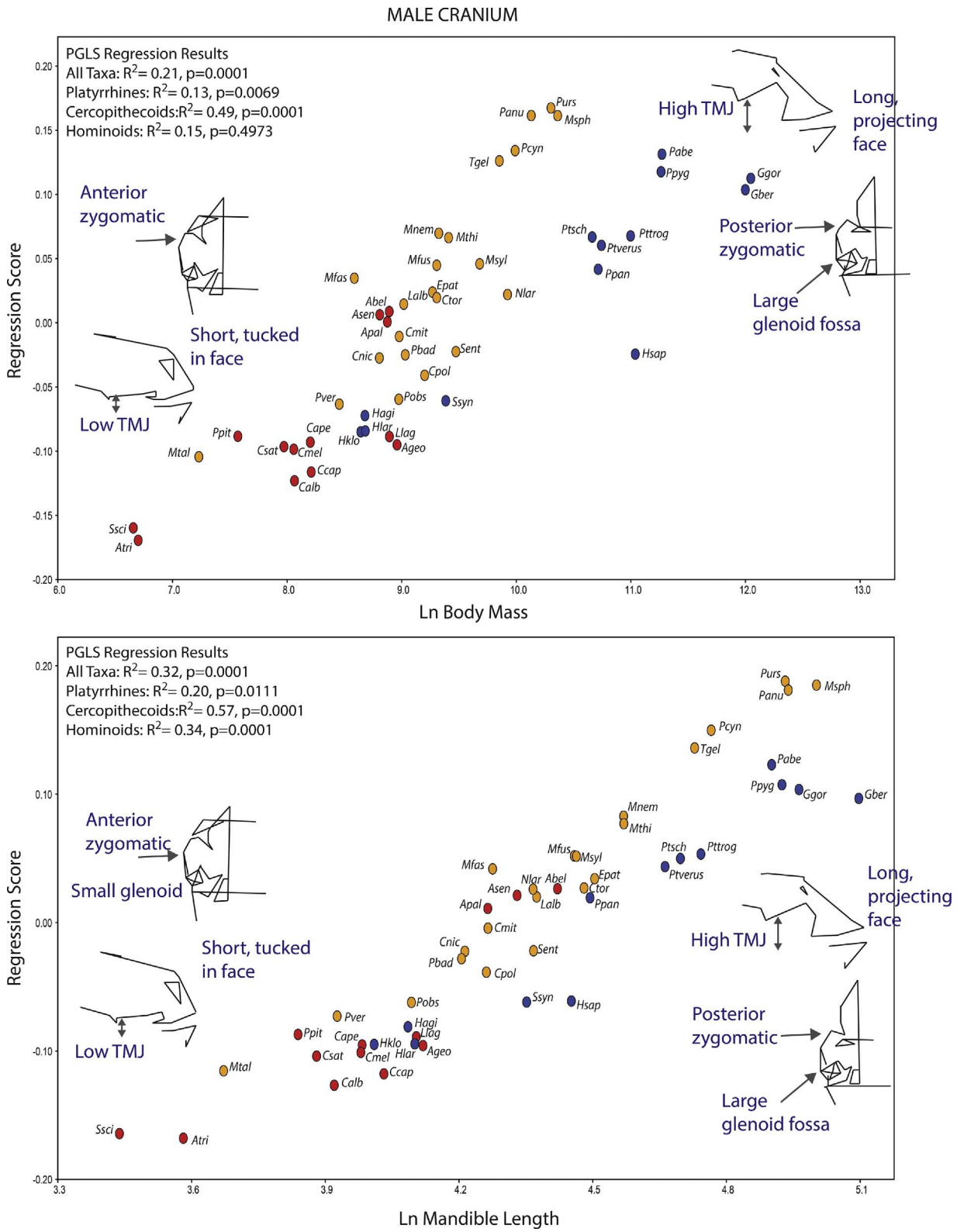

Fig. 6. Multivariate regression of the cranial configuration for the entire male sample on the natural log of body mass (top) and natural log of mandible length (bottom). Corresponding wireframe diagrams illustrate shape variation at the endpoints of the regression distribution.

Acknowledgements

Thanks go to Olga Panagiotopoulou and José Iriarte-Diaz for inviting me to contribute to this Special Issue and participate in the ICVM symposium. This research would not have been possible without all of the individuals and institutions that made their collections available: Eileen Westwig at the American Museum of Natural History, Mike Schweissing and Richard Kraft at the Department of Primatology at the

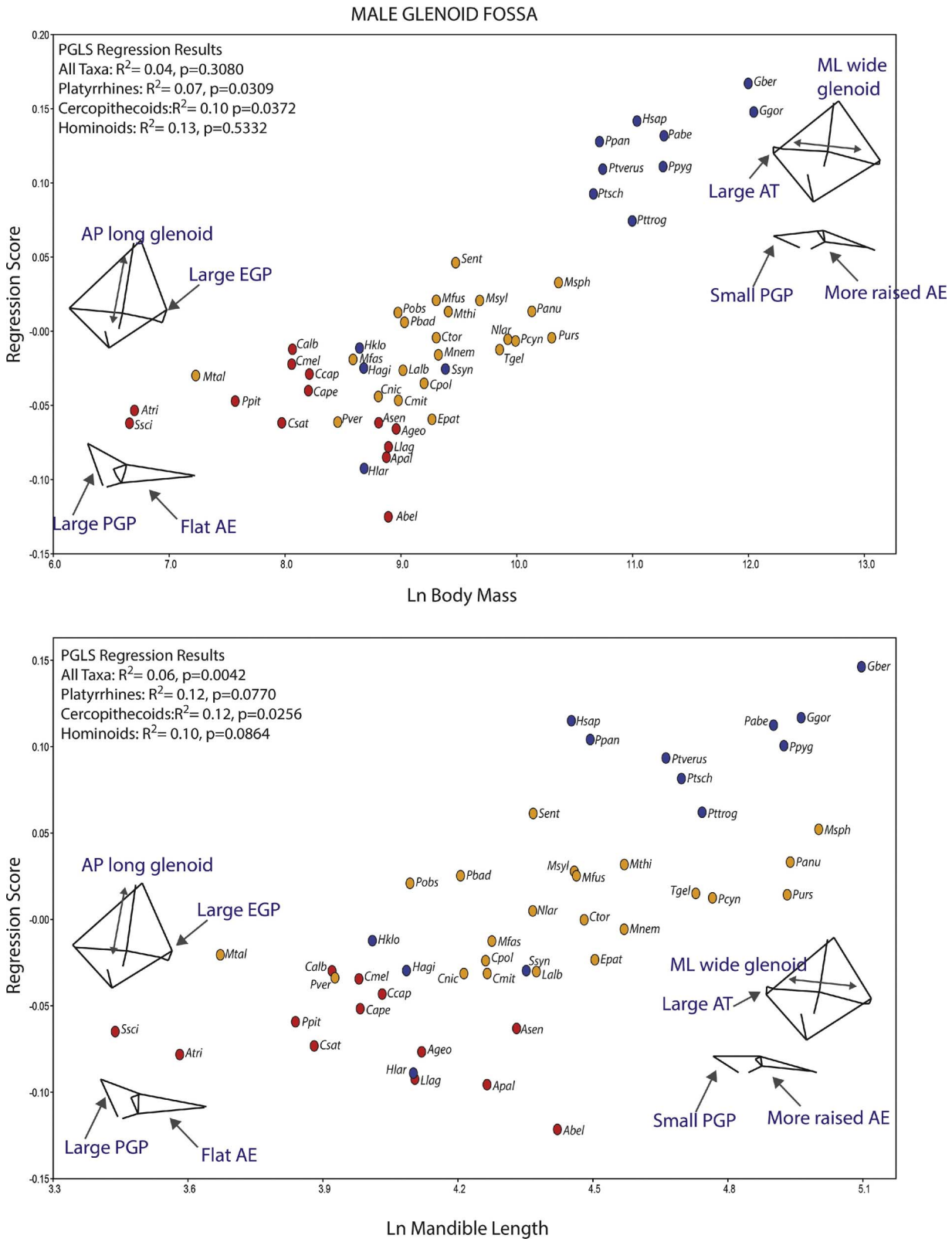

Fig. 7. Multivariate regression of the glenoid fossa configuration for the entire male sample on the natural log of body mass (top) and natural log of mandible length (bottom). Corresponding wireframe diagrams illustrate shape variation at the endpoints of the regression distribution.

State Collection of Anthropology and Paleoanatomy, Linda Gordon and Dave Hunt at the National Museum of Natural History, Bill Stanley at the Field Museum, and Emmanuel Gilissen and Wim Wendelen at the Royal Museum for Central Africa. Training in phylogenetic methods was provided by the AnthroTree Workshop, which was supported by the National Science Foundation (BCS-0923791) and the National Evolutionary Synthesis Center (NSF grant EF-09057606). This research was improved by feedback from Bill Kimbel, Gary Schwartz, Mark

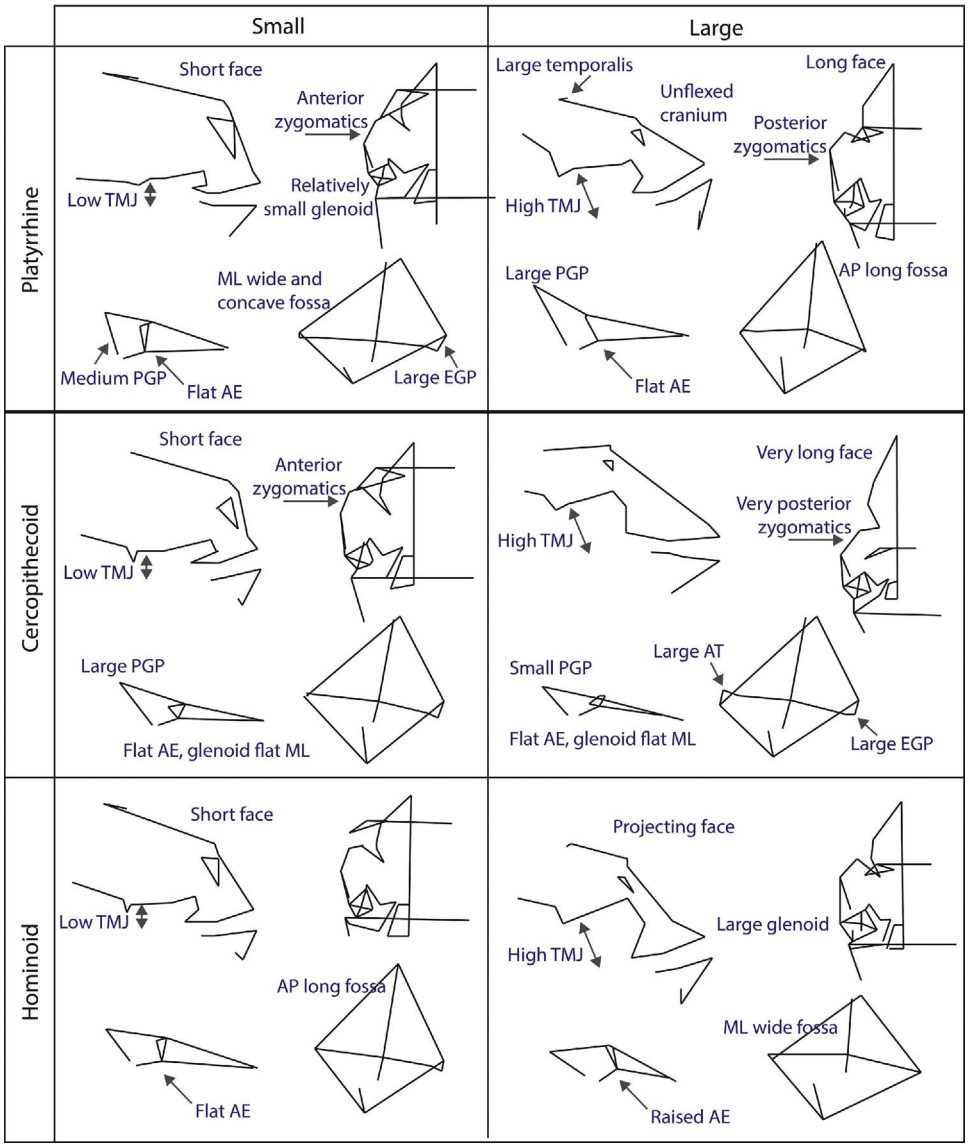

Fig. 8. Wireframe diagrams showing allometric shape variation for each clade within the sample. Wireframes are shown for both the cranial configuration and the glenoid fossa only configuration regressed on mandible length (males only). Corresponding regression statistics are provided in Table 10.

Spencer, Andrea Taylor, José Iriarte-Diaz, as well as two anonymous reviewers; all remaining faults are my own. Funding was provided for this research by the National Science Foundation (BCS-0752661), the Leakey Foundation, and Arizona State University.

Appendix A. Supplementary data

Supplementary data associated with this article can be found, in the online version, at http://dx.doi.org/10.1016/j.zool.2017.08.005.

References

Adams, D.C., Otárola-Castillo, E., 2013. Geomorph: an R package for the collection and analysis of geometric morphometric shape data. Methods Ecol. Evol. 4, 393–399.
Altmann, S.A., 1959. Field observations on a howling monkey society. J. Mammal. 40, 317–330.
Anapol, F., Lee, S., 1994. Morphological adaptation to diet in platyrrhine primates. Am. J. Phys. Anthropol. 94, 239–261.
Anapol, F., Shahnoor, N., Ross, C.F., 2008. Scaling of reduced physiologic cross-sectional area in primate muscles of mastication. In: Vinyard, C., Ravosa, M., Wall, C. (Eds.), Primate Craniofacial Function and Biology. Springer Science, New York, pp. 201–216.
Antón, S.C., 1999. Macaque masseter muscle: internal architecture, fiber length and cross-sectional area. Int. J. Prim. 20, 441–462.
Antón, S.C., 2000. Macaque pterygoid muscles: internal architecture, fiber length, and cross-sectional area. Int. J. Prim. 21, 131–156.
Arnold, C.L.J., Matthews, L., Nunn, C.L., 2010. The 10kTrees website: a new online resource for primate phylogeny. Evol. Anthropol. 19, 114–118.
Blomberg, S.P., Garland Jr., T., Ives, A.R., 2003. Testing for phylogenetic signal in comparative data: behavioral traits are more labile. Evolution 57, 717–745.
Bouvier, M., 1986a. A biomechanical analysis of mandibular scaling in Old World monkeys. Am. J. Phys. Anthropol. 69, 473–482.
Bouvier, M., 1986b. Biomechanical scaling of mandibular dimensions in New World monkeys. Int. J. Prim. 7, 551–567.
Cachel, S., 1984. Growth allometry in primate masticatory muscles. Arch. Oral Biol. 29, 287–293.
Carpenter, C.R., 1934. A field study of the behavior and social relations of howling monkeys. Comp. Psychol. Monog. 10, 1–168.
Constantino, P.J., 2007. Primate Masticatory Adaptations to Fracture-Resistant Foods. Ph.D. Thesis. George Washington University, Washington, D.C.
Copes, L.E., Schwartz, G.T., 2010. The scale of it all: postcanine tooth size, the taxon-level effect, and the universality of Gould's scaling law. Paleobiology 36, 188–203.
Corruccini, R., Henderson, A., 1978. Multivariate dental allometry in primates. Am. J. Phys. Anthropol. 48, 205–208.
Daegling, D.J., 2001. Biomechanical scaling of the hominoid mandibular symphysis. J. Morphol. 250, 12–23.
Dechow, P.C., Carlson, D.S., 1990. Occlusal force and craniofacial biomechanics during growth in rhesus monkeys. Am. J. Phys. Anthropol. 83, 219–237.
DuBrul, E.L., 1974. Origin and evolution of the oral apparatus. Front. Oral Physiol. 1, 1–30.
DuBrul, E.L., 1977. Early hominid feeding mechanisms. Am. J. Phys. Anthropol. 47, 305–320.

Enquist, B., Economo, E., Huxman, T., Allen, A., Ignace, D., Gillooly, J., 2003. Scaling metabolism from organisms to ecosystems. Nature 423, 639–642.
Felsenstein, J., 1985. Phylogenies and the comparative method. Am. Nat. 125, 1–15.
Fortelius, M., 1985. Ungulate cheek teeth: developmental, functional, and evolutionary interrelations. Acta Zool. Fennica 190, 1–76.
Freckleton, R.P., Harvey, P.H., Pagel, M., 2002. Phylogenetic analysis and comparative data: a test and review of evidence. Am. Nat. 160, 712–726.
Freeman, P.W., 1988. Frugivorous and animalivorous bats (Microchiroptera): dental and cranial adaptations. Biol. J. Linn. Soc. 33, 249–272.
Gould, S.J., 1975. On the scaling of tooth size in mammals. Am. Zool. 15, 351–362.
Grafen, A., 1989. The phylogenetic regression. Phil. Trans. Royal Soc. B 326, 119–157.
Greaves, W.S., 1974. Functional implications of mammalian jaw joint position. Forma et Functio 7, 363–376.
Greaves, W.S., 1978. The jaw lever system in ungulates: a new model. J. Zool. Lond. 184, 271–285.
Greaves, W.S., 1980. The mammalian jaw mechanism — the high glenoid cavity. Am. Nat. 116, 432–440.
Herring, S.W., Herring, S.E., 1974. The superficial masseter and gape in mammals. Am. Nat. 108, 561–576.
Hershkovitz, P., 1949. Mammals of northern Colombia. Preliminary report No. 4: Monkeys (Primates) with taxonomic revisions of some forms. Proc. US Nat. Mus. 98, 323–427.
Hill, W.C.O., 1962. Primates, Comparative Anatomy and Taxonomy, vol. V: Cebidae, Part B University Press, Edinburgh.
Hylander, W.L., 2006. Functional anatomy and biomechanics of the masticatory apparatus. In: Laskin, J.L., Greene, C.S., Hylander, W.L. (Eds.), Temporomandibular Disorders: An Evidenced Approach to Diagnosis and Treatment. Quintessence Pub. Co.; New York.
Hylander, W.L., 1975. Incisor size and diet in anthropoids with special reference to Cercopithecidae. Science 189, 1095–1098.
Hylander, W.L., 1979. An experimental analysis of temporomandibular joint reaction force in macaques. Am. J. Phys. Anthropol. 51, 433–456.
Hylander, W.L., 1985. Mandibular function and biomechanical stress and scaling. Am. Zool. 25, 315–330.
Hylander, W.L., 2013. The functional significance of canine reduction in early hominins. Am. J. Phys. Anthropol. 150, 247–259.
Hylander, W.L., Bays, R., 1979. An in vivo strain-gauge analysis of the squamosal-dentary joint reaction force during mastication and incisal biting in *Macaca mulatta* and *Macaca fascicularis*. Arch. Oral Biol. 24, 689–697.
Ives, A.R., Midford, P.E., Garland Jr., T., 2007. Within-species variation and measurement error in phylogenetic comparative methods. Syst. Biol. 56, 252–270.
Kay, R.F., 1975a. The functional adaptation of primate molar teeth. Am. J. Phys. Anthropol. 43, 195–216.
Kay, R.F., 1975b. Allometry and early hominids. Science 189, 61–63.
Kay, R.F., 1985. Dental evidence for the diet of *Australopithecus*. Ann. Rev. Anthropol. 14, 315–341.
Kay, R.F., Hylander, W., 1978. The dental structure of mammalian folivores with special reference to primates and Phalangeroidea (Marsupialia). In: Montgomary, G.G. (Ed.), The Biology of Arboreal Folivores. Smithsonian Institution Press, Washington DC, pp. 173–191.
Kleiber, M., 1932. Body size and metabolism. Hilgardia 61, 315–353.
Kleiber, M., 1947. Body size and metabolic rate. Phys. Rev. 27, 511–541.
Klingenberg, C.P., 2009. Morphometric integration and modularity in configurations of landmarks: tools for evaluating a priori hypotheses. Evol. Dev. 11, 405–421.
Lucas, P.W., 2004. Dental Functional Morphology: How Teeth Work. Cambridge University Press, New York.
Marshall, A.J., Wrangham, R.W., 2007. Evolutionary consequences of fallback foods. Int. J. Prim. 28, 1219–1235.
Maynard Smith, J., Savage, R.J.G., 1959. The mechanics of mammalian jaws. School Sci. Rev. 141, 289–301.
McGraw, W.S., Vick, A.E., Daegling, D.J., 2011. Sex and age differences in the diet and ingestive behaviors of sooty mangabeys (*Cercocebus atys*) in the Tai Forest Ivory Coast. Am. J. Phys. Anthropol. 144, 140–153.
McGraw, W.S., Vick, A.E., Daegling, D.J., 2014. Dietary variation and food hardness in sooty mangabeys (*Cercocebus atys*): implications for fallback foods and dental adaptation. Am. J. Phys. Anthropol. 154, 413–423.
McNab, B., 1988. Complications inherent in scaling the basal rate of metabolism in mammals. Quart. Rev. Biol. 63, 25–54.
McNab, B., 2003. Metabolism: ecology shapes bird bioenergetics. Nature 426, 620–621.
McNulty, K.P., Vinyard, C.J., 2015. Morphometry, geometry, function, and the future. Anat. Rec. 298, 328–333.
Moffett, B., 1966. The morphogenesis of the temporomandibular joint. Am. J. Orthodont. 52, 401–415.
Norconk, M.A., Wright, B.W., Conklin-Brittain, N.L., Vinyard, C.J., 2009. Mechanical and nutritional properties of food as factors in platyrrhine dietary adaptations. In: Garber, P.A., Estrada, A., Bicca-Marques, J.C., Heymann, E.W., Strier, K.B. (Eds.), South American Primates: Testing New Theories in the Study of Primate Behavior, Ecology, and Conservation. Springer Science, New York, pp. 279–319.
Nunn, C.L., Barton, R.A., 2001. Comparative methods for studying primate adaptation and allometry. Evol. Anth. 10, 81–98.
Pagel, M., 1999. Inferring the historical patterns of biological evolution. Nature 401, 877–884.
Perry, J.M.G., Hartstone-Rose, A., 2010. Maximum ingested food size in captive strepsirrhine primates: scaling and the effects of diet. Am. J. Phys. Anthropol. 142, 625–635.
Perry, J.M.G., Wall, C.E., 2008. Scaling of the chewing muscles in prosimians. In: Vinyard, C., Ravosa, M., Wall, C. (Eds.), Primate Craniofacial Function and Biology. Springer Science, New York, pp. 217–240.
Perry, J.M.G., Hartstone-Rose, A., Wall, C.E., 2011. The jaw adductors of strepsirrhines in relation to body size, diet, and ingested food size. Anat. Rec. 294, 712–728.
Perry, J.M.G., Bastian, M.L., St Clair, E., Hartstone-Rose, A., 2015. Maximum ingested food size in captive anthropoids. Am. J. Phys. Anthropol. 158, 92–104.
Peters, R.H., 1983. The Ecological Implications of Body Size. Cambridge University Press, Cambridge.
Pirie, C., 1978. Allometric scaling in the postcanine dentition with reference to primate diets. Primates 19, 583–591.
Plavcan, J.M., van Schaik, C.P., Kappeler, P.M., 1995. Competition, coalitions and canine size in primates. J. Hum. Evol. 28, 245–276.
Powell, P.L., Roy, R.R., Kanim, P., Bello, M.A., Edgerton, V.R., 1984. Predictability of skeletal muscle tension from architectural determinations in guinea pig hindlimbs. J. Appl. Physiol. 57, 1715–1721.
Ravosa, M.J., 1990. Functional assessment of subfamily variation in maxillomandibular morphology among Old World monkeys. Am. J. Phys. Anthropol. 82, 199–212.
Ravosa, M.J., 1991. Structural allometry of the prosimian mandibular corpus and symphysis. J. Hum. Evol. 20, 3–20.
Ravosa, M.J., 1996. Jaw morphology and function in living and fossil Old World monkeys. Int. J. Prim. 17, 909–932.
Ravosa, M.J., 2000. Size and scaling in the mandible of living and extinct apes. Folia Primatol. 71, 305–322.
Rayner, J.M.V., 1985. Linear relations in biomechanics: the statistics of scaling functions. J. Zool. Lond. A 206, 415–439.
Revell, L.J., 2012. phytools: an R package for phylogenetic comparative biology (and other things). Methods Ecol. Evol. 3, 217–223.
Rice, W.R., 1989. Analyzing tables of statistical tests. Evolution 43, 223–225.
Ross, C.F., Iriarte-Diaz, J., 2014. What does feeding system morphology tell us about feeding? Evol. Anthropol. 23, 105–120.
Ross, C.F., Washington, R.L., Eckhardt, A., Reed, D.A., Vogel, E., Dominy, N., Machanda, Z., 2009a. Ecological consequences of scaling of chew cycle duration and daily feeding time in Primates. J. Hum. Evol. 56, 570–585.
Ross, C.F., Reed, D.A., Washington, R.L., Eckhardt, A., Anapol, F., Shahnoor, N., 2009b. Scaling of chew cycle duration in primates. Am. J. Phys. Anthropol. 138, 30–44.
Sailer, L.D., Gaulin, S.J.C., Boster, J.S., Kurland, J.A., 1985. Measuring the relationship between dietary quality and body size in primates. Primates 26, 14–27.
Savage, V.M., Gillooly, J.F., Woodruff, W.H., West, G.B., Allen, A.P., Enquist, B.J., Brown, J.H., 2004. The predominance of quarter-power scaling in biology. Funct. Ecol. 18, 257–282.
Schmidt-Nielsen, K., 1984. Scaling: Why is Animal Size So Important? Cambridge University Press, Cambridge.
Scott, J.E., 2011. Folivory, frugivory, and postcanine size in the Cercopithecoidea revisited. Am. J. Phys. Anthropol. 146, 20–27.
Scott, J.E., 2012. Molar size and diet in the Strepsirrhini: implications for size-adjustment in studies of primate dental adaptation. J. Hum. Evol. 63, 796–804.
Sicher, H., 1951. The Temporomandibular Joint. Charles C. Thomas Company, Springfield.
Singleton, M., 2005. Functional shape variation in the cercopithecine masticatory complex. In: Slice, D.E. (Ed.), Modern Morphometrics in Physical Anthropology. Kluwer Academic/Plenum Publishers, New York, pp. 319–348.
Smith, R.J., 1983. The mandibular corpus of female primates: taxonomic, dietary, and allometric correlates of interspecific variations in size and shape. Am. J. Phys. Anthropol. 61, 315–330.
Smith, R.J., 1993. Categories of allometry: body size versus biomechanics. J. Hum. Evol. 24, 173–182.
Smith, R.J., 2009. Use and misuse of the reduced major axis for line-fitting. Am. J. Phys. Anthropol. 140, 476–486.
Smith, R.J., Jungers, W.L., 1997. Body mass in comparative primatology. J. Hum. Evol. 32, 523–559.
Smith, R.J., Petersen, C.E., Gipe, D.P., 1983. Size and shape of the mandibular condyle in primates. J. Morphol. 177, 59–68.
Sokal, R.R., Rohlf, F.J., 1995. Biometry: The Principles and Practice of Statistics in Biological Research, 3rd ed. W. H. Freeman and Co., New York.
Spencer, M.A., 1995. Masticatory System Configuration and Diet in Anthropoid Primates. Ph.D. Thesis. State University of New York, Stony Brook.
Sun, Z., Liu, Z.J., Herring, S.W., 2002.. Movement of temporomandibular joint tissues during mastication and passive manipulation in miniature pigs. Arch. Oral Biol. 47, 293–305.
Taylor, A.B., 2002. Masticatory form and function in the African apes. Am. J. Phys. Anthropol. 117, 133–156.
Taylor, A.B., 2005. A comparative analysis of temporomandibular joint morphology in the African apes. J. Hum. Evol. 48, 555–574.
Taylor, A.B., 2006. Feeding behavior, diet, and the functional consequences of jaw form in orangutans, with implications for the evolution of *Pongo*. J. Hum. Evol. 50, 377–393.
Taylor, A.B., Vinyard, C.J., 2013. The relationships among jaw-muscle fiber architecture, jaw morphology, and feeding behavior in extant apes and modern humans. Am. J. Phys. Anthropol. 151, 120–134.
Taylor, A.B., Vogel, E.R., Dominy, N.J., 2008. Food material properties and mandibular load resistance abilities in large-bodied hominoids. J. Hum. Evol. 55, 604–616.
Taylor, A.B., Yuan, T., Ross, C.F., Vinyard, C.J., 2015. Jaw-muscle force and excursion scale with negative allometry in platyrrhine primates. Am. J. Phys. Anthropol. 158, 242–256.
Terhune, C.E., 2010. The Temporomandibular Joint in Anthropoid Primates; Functional, Allometric, and Phylogenetic Influences. Ph.D. Thesis. Arizona State University,

Tempe, AZ.
Terhune, C.E., 2011a. Modeling the biomechanics of articular eminence function in anthropoid primates. J. Anat. 219, 551–564.
Terhune, C.E., 2011b. Dietary correlates of temporomandibular joint morphology in New World primates. J. Hum. Evol. 61, 583–596.
Terhune, C.E., 2013. Dietary correlates of temporomandibular joint morphology in the great apes. Am. J. Phys. Anthropol. 150, 260–272.
Terhune, C.E., Hylander, W.L., Vinyard, C.J., Taylor, A.B., 2015. Jaw-muscle architecture and mandibular morphology influence relative maximum jaw gapes in the sexually dimorphic *Macaca fascicularis*. J. Hum. Evol. 82, 145–158.
Vinyard, C.J., 1999. Temporomandibular Joint Morphology and Function in Strepsirrhine and Eocene Primates. Ph.D. Thesis. Northwestern University, Evanston, IL.
Vinyard, C.J., 2008. Putting shape to work: making functional interpretations of masticatory apparatus shapes in primates. In: Vinyard, C.J., Ravosa, M.J., Wall, C.E. (Eds.), Primate Craniofacial Function and Biology. Springer Science, New York, pp. 357–386.
Vinyard, C.J., Hanna, J., 2005. Molar scaling in strepsirrhine primates. J. Hum. Evol. 49, 241–269.
Vinyard, C.J., Ravosa, M.J., 1998. Ontogeny, function, and scaling of the mandibular symphysis in papionin primates. J. Morphol. 235, 157–175.
Vinyard, C.J., Wall, C.E., Williams, S.H., Hylander, W.L., 2003. Comparative functional analysis of skull morphology of tree-gouging primates. Am. J. Phys. Anthropol. 120, 153–170.
Vinyard, C.J., Taylor, A.B., Teaford, M.F., Glander, K.E., Ravosa, M.J., Rossie, J.B., Ryan, T.M., Williams, S.H., 2011. Are we looking for loads in all the right places? New research directions for studying the masticatory apparatus of New World monkeys. Anat. Rec. 294, 2140–2157.
Vogel, E.R., van Woerden, J.T., Lucas, P.W., Utami Atmoko, S.S., van Schaik, C.P., Dominy, N.J., 2008. Functional ecology and evolution of hominoid molar enamel thickness: *Pan troglodytes schweinfurthii*and *Pongo pygmaeus wurmbii*. J. Hum. Evol. 55, 60–74.
Wall, C.E., 1995. Form and Function of the Temporomandibular Joint in Anthropoid Primates. Ph.D. Thesis. State University of New York, Stony Brook.
Wall, C.E., 1997. The expanded mandibular condyle of Megaladapidae. Am. J. Phys. Anthropol. 103, 263–276.
Wall, C.E., 1999. A model of temporomandibular joint function in anthropoid primates based on condylar movements during mastication. Am. J. Phys. Anthropol. 109, 67–88.
Ward, S.C., Molnar, S., 1980. Experimental stress analysis of topographic diversity in early hominid gnathic morphology. Am. J. Phys. Anthropol. 53, 383–395.
Watanabe, T., 1982. Mandible/basihyal relationships in red howler monkeys (*Alouatta seniculus*): a craniometrical approach. Primates 23, 105–129.
White, C.R., Seymour, R.S., 2003. Mammalian basal metabolic rate is proportional to body mass$^{2/3}$. Proc. Nat. Acad. Sci. 100, 4046–4049.
White, C.R., Blackburn, T.M., Seymour, R.S., 2009. Phylogenetically informed analysis of the allometry of mammalian basal metabolic rate supports neither geometric nor quarter-power scaling. Evolution 63, 2658–2667.
Williams, S.H., Wright, B.W., Truong, V.D., Daubert, C.R., Vinyard, C.J., 2005. Mechanical properties of foods used in experimental studies of primate masticatory function. Am. J. Prim. 67, 329–346.
Wright, B.W., 2005. Craniodental biomechanics and dietary toughness in the genus *Cebus*. J. Hum. Evol. 48, 473–492.